

# Absorption line indices from high resolution spectra. I. New Response Functions

R. Tantalo<sup>1</sup>, C. Chiosi<sup>1</sup>, U. Munari<sup>2</sup>, L. Piovan<sup>1</sup>, & R. Sordo<sup>2</sup>

<sup>1</sup> Department of Astronomy, University of Padova, Vicolo dell’Osservatorio 2, 35122 Padova, Italy

<sup>2</sup> INAF, Astronomical Observatory of Padova, Vicolo Osservatorio 5, 35122 Padova, Italy

E-mail: chiosi@pd.astro.it; ulisse@pd.astro.it; piovan@pd.astro.it; sordo@pd.astro.it; tantalo@pd.astro.it

Submitted: May 2004

## ABSTRACT

Basing on the huge library of 1 Å resolution spectra calculated by Munari et al. (2004) over a large range of  $\log T_{\text{eff}}$ ,  $\log g$ , [Fe/H] and both for solar and  $\alpha$ -enhanced abundance ratios ( $[\text{X}_{\text{el}}/\text{Fe}]$ ), we present theoretical absorption line indices on the Lick system. Firstly we derive the so-called *Response Functions* ( $\mathcal{RF}$ s) of Tripicco & Bell (1995) for a wide range of  $\log T_{\text{eff}}$ ,  $\log g$ , [Fe/H], and  $[\alpha/\text{Fe}] = +0.4$ . The  $\mathcal{RF}$ s are commonly used to correct indices with solar  $[\alpha/\text{Fe}]$  ratios to indices with  $[\alpha/\text{Fe}] > 0$ . Not only the  $\mathcal{RF}$ s vary with the type of star but also with the metallicity. Secondly, with the aid of this and the *Fitting Functions* ( $\mathcal{FF}$ s) of Worthey et al. (1994), we derive the indices for Single Stellar Populations and compare them with those obtained by previous authors, e.g. Tantalo & Chiosi (2004a). The new  $\mathcal{RF}$ s not only supersede the old ones by Tripicco & Bell (1995), but also confirm that method adopted by Tantalo & Chiosi (2004a) to include the effect of  $\alpha$ -enhancement was correct, and clearly show that also  $H_{\beta}$  increases with the degree of enhancement. All this lends support to the suggestion made by Tantalo & Chiosi (2004b) that a significant part of the scatter along the  $H_{\beta}$  axis shown by early-type galaxies of the Local Universe in the  $H_{\beta}$  vs. [Mg/Fe] plane (and similar) could be due to a spread in the mean enhancement factor from galaxy to galaxy and only occasionally to recent episodes of star formation. Finally, we present preliminary indices on the same system directly measured on the theoretical 1 Å resolution spectra. The analysis is still preliminary because much narrower spacing in  $T_{\text{eff}}$  and  $\log g$  than the one for the subset of the large library of Munari et al. (2004) we have adopted is indeed required. Work is in progress to include the desired spacing in the atmospheric parameters ( $T_{\text{eff}}$ ,  $\log g$ , and [Fe/H] or  $[\text{Z}/\text{Z}_{\odot}]$ ).

**Key words:** Galaxies: spectroscopy – Galaxies: metallicities

## 1 INTRODUCTION

The Lick system of absorption line indices developed over the years by Burstein et al. (1984), Faber et al. (1985), Worthey (1992), Worthey et al. (1992), Worthey et al. (1994), and Worthey (1994) was designed to infer the age and the metallicity of stellar systems, early-type galaxies in particular.

The Lick indices seem to have the potential of partially resolving the *age-metallicity degeneracy* that is long known to affect the spectral energy distribution of stellar populations (Renzini & Buzzoni 1986)<sup>1</sup>. Thanks to it, an extensive use of the Lick system of indices has been made

by many authors (Bressan et al. 1996; Tantalo 1998; Tantalo et al. 1998; Trager et al. 2000b,a; Kuntschner 1998; Kuntschner & Davies 1998; Jørgensen 1999; Kuntschner 2000; Poggianti et al. 2001; Kuntschner et al. 2001; Vazdekis et al. 2001; Davies et al. 2001; Maraston et al. 2003; Thomas et al. 2003a,b; Thomas & Maraston 2003; Tantalo & Chiosi 2004a). The main result of all those studies is that even in early-type galaxies some recent episodes of star formation ought to occur in order to explain the large scatter shown by the observational data for indices like  $H_{\beta}$  commonly thought to be sensitive to the turn-off stars and consequently to the age.

The problem is, however, further complicated by a third parameter, i.e. the abundance ratios  $[\alpha/\text{Fe}]$  (where  $\alpha$  stands for all chemical elements produced by  $\alpha$ -captures on lighter nuclei). Absorption line indices like  $\text{Mg}_2$  and  $\langle \text{Fe} \rangle$  measured

<sup>1</sup> An old metal-poor stellar population may happen to have the same spectral energy distribution of a young metal-rich one.

in the central regions of galaxies are known to vary passing from one galaxy to another (González 1993; Trager et al. 2000b,a). Looking at the correlation between  $Mg_2$  and  $\langle Fe \rangle$  (or similar indices) for the galaxies in the above quoted samples,  $Mg_2$  increases faster than  $\langle Fe \rangle$ , which is interpreted as due to enhancement of  $\alpha$ -elements in some galaxies. In addition to this, since the classical paper by Burstein et al. (1988), the index  $Mg_2$  is known to increase with the velocity dispersion (and hence mass and luminosity) of the galaxy. Standing on this body of data the conviction arose that the degree of enhancement in  $\alpha$ -elements ought to increase passing from dwarf to massive early-type galaxies (Faber et al. 1992; Worthey et al. 1994; Matteucci 1994, 1997; Matteucci et al. 1998). These findings strongly bear on the theory of galaxy formation as super-solar  $[\alpha/Fe]$  ratios require rather short star-formation time scales (see for instance the discussion of this topic by Chiosi & Carraro (2002)) and the correlation with the velocity dispersion requires that the star formation time scale should get longer at decreasing galaxy mass, in contrast with the standard supernova driven galactic wind model by Larson (1974), and instead supported by the N-Body-Tree-SPH models of early-type galaxies by Chiosi & Carraro (2002).

In presence of  $\alpha$ -enhanced chemical compositions, ages and metallicities of early-type galaxies should be derived from indices in which  $\alpha$ -enhancement is included. As long ago noticed by Worthey et al. (1992) and Weiss et al. (1995), indices for  $\alpha$ -enhanced chemical mixtures of given total metallicity are expected to differ from those of the standard case. On one hand this spurred new generations of stellar models, isochrones, SSPs with  $\alpha$ -enhanced mixtures (Salasnich et al. 2000) and on the other hand led to many attempts of increasing complexity to simultaneously derive, from fitting the observational indices to their theoretical counterparts, the age, metallicity and degree of enhancement (Tantalo et al. 1998; Trager et al. 2000b,a; Maraston et al. 2003; Thomas et al. 2003a,b; Thomas & Maraston 2003; Tantalo & Chiosi 2004a). The formal solution for ages, metallicities and  $[\alpha/Fe]$  ratios based on large samples of galaxies, e.g. the Trager (1997) list, once more yields a large range of ages, metallicities, and abundance ratios, as amply discussed by Tantalo & Chiosi (2004a, TC04a).

Although the picture emerging from the above studies is a convincing one, there are still several points of weakness intrinsic even to the state-of-the-art theoretical indices that force us to reconsider the whole problem. Let us examine in some detail (i) the foundations of the Lick indices; (ii) the various steps that are required to derive theoretical indices and their dependence on age, metallicity, and degree of enhancement; (iii) the current method to estimate these parameters from the indices; (iv) and finally shortly comment on a few points of controversy among different groups.

- The information contained in the stellar spectra concerning the effective temperature ( $T_{\text{eff}}$ ), gravity ( $\log g$ ), and chemical composition (mainly the parameter  $[\text{Fe}/\text{H}]$ ) has been coded in a system of indices measuring the strength of atomic and molecular lines (see Section 2). The Lick indices are defined and measured on a sample of stellar spectra with fixed mean resolution of 8 Å which in most cases is different from the resolution of theoretical spectra on which

the indices are calculated. This simple fact will turn out to be a major reason of uncertainty.

- To overcome the above difficulty and to make possible the general use of the Lick indices, Worthey et al. (1994) introduced the concept of the so-called Fitting Functions ( $\mathcal{FFs}$ ). The indices for a large sample of stars with known atmospheric parameters ( $T_{\text{eff}}$ ,  $\log g$  and  $[\text{Fe}/\text{H}]$ ) are measured and then expressed as empirical polynomial fits as functions of these parameters. The major drawback with the  $\mathcal{FFs}$  is that they encompass a limited range of values in particular as far as  $[\text{Fe}/\text{H}]$  is concerned. The sample of stars indeed was collected from the solar vicinity even if attempts to extend it to lower metallicities have been made (Idiart & de Freitas-Pacheco (1995), Cenarro et al. (2001, 2002)). Metallicities much higher than those in the solar vicinity are simply not included for obvious reasons. A new library is also available with unprecedented coverage of atmospheric parameters by Sánchez-Blázquez et al. (2003); Sanchez-Blazquez & et al. (2004).

- Despite it was long known that Magnesium is perhaps enhanced with respect to Iron ( $[\text{Mg}/\text{Fe}] > 0$ ) in giant elliptical galaxies, see e.g. Worthey et al. (1992) and above, the collection of stellar spectra and  $\mathcal{FFs}$  in turn did not allow for non-standard abundance ratios in the chemical composition. Only occasionally and for a few indices, e.g.  $Mg_2$  and  $NaD$ ,  $\mathcal{FFs}$  including the effect of non-standard abundance ratios have been proposed, e.g. Borges et al. (1995).

- A milestone along the road was put by Tripicco & Bell (1995, TB95) who have modeled synthetic spectra of high resolution (0.1 Å), degraded them to the mean 8 Å resolution of the Lick system, and derived from them the indices for three prototype stars, namely a cool-dwarf, a turn-off, and a cool-giant along a 5 Gyr isochrone matching the CMD of M67 (in other words for three different combinations of  $T_{\text{eff}}$  and  $\log g$ ). Even more important here, they studied the response of the indices produced by changes in the abundance ratios of individual elements. In other words, thanks to their  $\mathcal{RFs}$  it was possible to evaluate the effect of abundance ratios different from solar.

- With the aid of the TB95  $\mathcal{RFs}$  and suitable algorithms, the indices with solar abundance ratios have been transformed into those for non solar abundance ratios. The algorithms in use are not unique thus leading to uncertain results (see TC04a for more details).

- Passing now from individual stars to star clusters, reduced here to Single Stellar Populations (SSPs), and galaxies (manifolds of SSPs), the derivation of theoretical indices (and spectra, magnitudes, and broad-band colours) is even more complicate because other ingredients intervene: (i) the construction of realistic isochrones for SSPs including all evolutionary phases (even the unusual ones that are known to appear at very high metallicities, see Bressan et al. (1994) and TC04a); (ii) the initial mass function; (iii) and finally in the case of galaxies, the past history of star formation and chemical enrichment weighing the contribution from stellar populations of different age and chemical compositions (see e.g. Bressan et al. 1994, for all details). It is worth commenting here that galaxy indices are almost always compared to SSP indices thus neglecting the mix of stellar populations and missing important contributions from some peculiar components. For instance an old SSP of very high metallicity and/or a very old SSP of extremely low metal

content, would possess strong  $H_\beta$  thus mimicking a young SSP of normal metallicity (see TC04a for more details). Integrated indices for model galaxies have been occasionally calculated and used (Tantalo 1998), but never systematically applied to this kind of analysis. This is a point that should be carefully investigated and kept in mind when comparing data with theory.

If for solar abundance ratios the dependence of the indices on age and metallicity is currently on a rather solid ground but for the effect of some unusual phases of stellar evolution, the same does not happen for non solar abundance ratios because it is still highly controversial how some indices ( $H_\beta$ , in particular) at given age and total metallicity would respond to changes in the abundance ratios. According to TC04a, SSPs of the same age and metallicity but different degrees of enhancement in  $\alpha$ -elements may have significantly different  $H_\beta$ : in brief keeping age and metallicity constant,  $H_\beta$  should increase at increasing degree of enhancement (see the discussion in Section 3.2 for more details). Basing on this, Tantalo & Chiosi (2004b) suggested an alternative, complementary interpretation of the large scatter in  $H_\beta$  shown by early-type galaxies of the local Universe in two-indices diagnostic planes like  $H_\beta$  vs.  $[\text{Mg}/\text{Fe}]$ . Quickly summarizing their study: (i) Most likely, the majority of galaxies (those with  $H_\beta \leq 2$ ) are very old objects of the same age (say about 13 Gyr) but a different degree of enhancement. (ii) Only for galaxies with  $H_\beta > 2$ , the presence of secondary star forming activity ought to be invoked.

High resolution synthetic spectra can greatly alleviate the above difficulties and shed light on these important issues, which is the aim of our study. The plan of the paper is as follows. Section 2 deals with the theory of absorption line indices; Section 2.1 summarizes their definition for a single star; Section 2.2 derives the *enhancement factor* for a mixture in which the abundance of  $\alpha$ -elements with respect to that of Fe is enhanced as compared to the Solar Mix; Section 2.3 recalls the dependence of the  $\mathcal{FF}$ s of the Lick system on the main stellar parameters, comments on the fact that they are based on solar-scaled chemical compositions, and shortly describes the  $\mathcal{FF}$ s by Borges et al. (1995) in which for some indices the effect of enhancing  $\alpha$ -elements is taken into account; finally Section 2.4 shortly reviews the method of the  $\mathcal{RF}$ s by TB95 and current algorithms that are adopted to transfer solar-scaled indices into the corresponding ones with  $\alpha$ -enhancement. In Section 3 we present our new  $\mathcal{RF}$ s. They closely follow the definition by TB95 but are now derived from high resolution synthetic spectra for a wide volume of the parameter space. The synthetic spectral library in use is shortly described in Section 3.1, whereas the indices for the calibrating stars are given in Section 3.2 and in appendix. The covered  $T_{\text{eff}}$  and  $\log g$  extend nearly across the whole HR-Diagram of real stars, the metallicity goes  $[\text{Z}/\text{Z}_\odot] = -2.0$  to 0.5 for spectra with  $[\alpha/\text{Fe}] = 0$  and up to -0.5 for spectra with  $[\alpha/\text{Fe}] = +0.4$ . These indices constitute the backbone of the new grid of TB95-like  $\mathcal{RF}$ s given in Section 3.3. Owing to the large body of data on the Lick system, it is worth providing indices calculated with the classical  $\mathcal{FF}$ s and the new  $\mathcal{RF}$ s to pass from solar to  $\alpha$ -enhanced mixtures. These indices are immediately comparable to most of observational data in literature. This is the subject of Section 4. We start by shortly recalling the index

definition for SSPs and the library of stellar spectra with medium resolution specifically used to this purpose (Section 4.1) and summarising the sources of stellar models and isochrones (Section 4.2). With the aid of the new  $\mathcal{RF}$ s we calculate absorption line indices for SSPs at varying metallicity, degree of enhancement, and age. The results are presented in Section 4.3 and compared to those by previous sources, e.g. TC04a, in Section 4.4. The increase of  $H_\beta$  with the degree of enhancement is fully confirmed, thus lending support to the conclusion reached by TC04a. Finally in Section 4.5 we compare the new indices with the observational data for Galactic Globular Clusters. As final exploratory step of this study, and for the first time in literature, in Section 5 we present indices derived directly from the theoretical 1 Å resolution spectra without passing through the  $\mathcal{FF}$ s and the  $\mathcal{RF}$ s. Firstly we calculate the indices for the calibrating stars and compare them with the corresponding ones, roughly at the same atmospheric parameters for a selected sample of stars in STELIB (Section 5.1). Then we derive the indices for SSPs by means of the standard spectral synthesis technique by interpolating the high resolution spectra as function of  $T_{\text{eff}}$  and  $\log g$  (at given metallicity and degree of enhancement). For the time being we prefer not to interpolate the spectra in metallicity and degree of enhancement, and wait for a wider grid to become available. The new indices are given in Section 5.2. Even if the current temperature-gravity grid is perhaps too coarse for this purpose, the results are acceptable. They will soon improve by adopting a library of spectra with much finer coverage of the temperature/gravity space. Finally, a summary of the results of this study and some concluding remarks are presented in Section 6.

## 2 THEORY OF ABSORPTION LINE INDICES

### 2.1 Definition

The definition of an absorption line index with pass-band  $\Delta_\lambda$  is different according to whether it is measured in equivalent width (EW) or magnitude (Mag). Those in EW are defined as

$$I_l = \Delta_\lambda \left( 1 - \frac{F_l}{F_c} \right) \quad (1)$$

where  $F_l$  and  $F_c$  are the fluxes in the line and pseudo-continuum, respectively (see Fig. 6). The flux  $F_c$  is calculated by interpolating to the central wavelength of the absorption line, the fluxes in the midpoints of the red and blue pseudo-continua bracketing the line (Worley et al. 1994). The definition of indices expressed in Mag is

$$I_l = -2.5 \log \left( \frac{F_l}{F_c} \right) \quad (2)$$

The pass-bands adopted for each index are listed in Table 1. Since the Lick system of indices (Burstein et al. 1984; Faber et al. 1985; Worley et al. 1994) stands on a spectra library with resolution of about 8 Å, whereas most of the spectral libraries in use have a different resolution, the straightforward application of eqns. (1) and (2) is not possible. To overcome

**Table 1.** 25 Absorption line indices on the Lick system: the pass-bands, and the  $\lambda 4000$  break.

Index	Type	Central Band		Blue Continuum		Red Continuum	
CN <sub>1</sub>	Mag	4142.125	4177.125	4080.125	4117.625	4244.125	4284.125
CN <sub>2</sub>	Mag	4142.125	4177.125	4083.875	4096.375	4244.125	4284.125
Ca4227	EW	4222.250	4234.750	4211.000	4219.750	4241.000	4251.000
G4300	EW	4281.375	4316.375	4266.375	4282.625	4318.875	4335.125
Fe4383	EW	4369.125	4420.375	4359.125	4370.375	4442.875	4455.375
Ca4455	EW	4452.125	4474.625	4445.875	4454.625	4477.125	4492.125
Fe4531	EW	4514.250	4559.250	4504.250	4514.250	4560.500	4579.250
C24668	EW	4634.000	4720.250	4611.500	4630.250	4742.750	4756.500
H <sub><math>\beta</math></sub>	EW	4847.875	4876.625	4827.875	4847.875	4876.625	4891.625
Fe5015	EW	4977.750	5054.000	4946.500	4977.750	5054.000	5065.250
Mg <sub>1</sub>	Mag	5069.125	5134.125	4895.125	4957.625	5301.125	5366.125
Mg <sub>2</sub>	Mag	5154.125	5196.625	4895.125	4957.625	5301.125	5366.125
Mg <sub>b</sub>	EW	5160.125	5192.625	5142.625	5161.375	5191.375	5206.375
Fe5270	EW	5245.650	5285.650	5233.150	5248.150	5285.650	5318.150
Fe5335	EW	5312.125	5352.125	5304.625	5315.875	5353.375	5363.375
Fe5406	EW	5387.500	5415.000	5376.250	5387.500	5415.000	5425.000
Fe5709	EW	5696.625	5720.375	5672.875	5696.625	5722.875	5736.625
Fe5782	EW	5776.625	5796.625	5765.375	5775.375	5797.875	5811.625
NaD	EW	5876.875	5909.375	5860.625	5875.625	5922.125	5948.125
TiO <sub>1</sub>	Mag	5936.625	5994.125	5816.625	5849.125	6038.625	6103.625
TiO <sub>2</sub>	Mag	6189.625	6272.125	6066.625	6141.625	6372.625	6415.125
H <sub><math>\delta</math>A</sub>	EW	4083.500	4122.250	4041.600	4079.750	4128.500	4161.000
H <sub><math>\gamma</math>A</sub>	EW	4319.750	4363.500	4283.500	4319.750	4367.250	4419.750
H <sub><math>\delta</math>F</sub>	EW	4091.000	4112.250	4057.250	4088.500	4114.750	4137.250
H <sub><math>\gamma</math>F</sub>	EW	4331.250	4352.250	4283.500	4319.750	4354.750	4384.750
D <sub>4000</sub>				3750.000	3950.000	4050.000	4250.000

this problem, the  $\mathcal{FF}$ s are introduced. They express the indices measured on the observed spectra of a large number of stars with known  $\log g$ ,  $T_{\text{eff}}$ , and chemical composition as functions of these parameters (Worley et al. 1994).

We also add the index D<sub>4000</sub> centered at the 4000 Å break. It is defined as the ratio of the average flux  $F_{\nu}$  (in  $\text{erg sec}^{-1} \text{cm}^{-2} \text{Hz}^{-1}$ ) in two bands at the long- and short-wavelength side of the discontinuity (Bruzual 1983), i.e.

$$D_{4000} = \frac{\lambda_2^b - \lambda_1^b}{\lambda_2^r - \lambda_1^r} \frac{\int_{\lambda_1^b}^{\lambda_2^r} F_{\nu} d\lambda}{\int_{\lambda_1^b}^{\lambda_2^r} F_{\nu} d\lambda}$$

The blue and red pass-bands are given in Table 1.

## 2.2 $\alpha$ -enhanced chemical compositions

The degree of enhancement in  $\alpha$ -elements of a chemical mixture is measured by the so-called *total enhancement parameter*  $\Gamma$ , to distinguish it from the enhancement in individual species. Let us take a certain mixture of elements with total metallicity  $Z$  (sum of all elements heavier than He), denote with  $N_j$  the number density of the generic element  $j$  with mass abundance  $X_j$  ( $N_j = \rho N_0 X_j / A_j$ , where  $\rho$  is the mass density,  $N_0$  is the Avogadro number, and  $A_j$  is the mass number) and define the quantity  $A_j$

$$A_j = \log \left( \frac{N_j}{N_H} \right) + 12 \quad (3)$$

Ignoring elements from H to He, in this mixture  $\sum_j X_j = Z$  by definition. The abundance by mass with respect to Fe is given by

$$\left[ \frac{X_j}{X_{Fe}} \right] = \log \left( \frac{X_j}{X_{Fe}} \right) - \log \left( \frac{X_j}{X_{Fe}} \right)_{\odot} \quad (4)$$

or in terms of  $A_j$

$$\left[ \frac{X_j}{X_{Fe}} \right] = (A_{X_j} - A_{X_j}^{\odot}) - (A_{Fe} - A_{Fe}^{\odot}) \quad (5)$$

Keeping constant the number density of Fe, i.e.  $(A_{Fe} - A_{Fe}^{\odot}) = 0$  and changing other elements (enhancement), we get

$$A_j^{enh} = \left[ \frac{X_j}{X_{Fe}} \right] + A_j^{\odot} \quad (6)$$

Inserting the adopted  $[X_j/X_{Fe}]$  and the solar values for  $A_j^{\odot}$  by Grevesse & Sauval (1998), respectively, from eqn. (3) we can calculate the new abundances by mass for any pattern of  $\alpha$ -enhanced elements. In general, the sum of the  $X_j$  will be different from  $Z$ . The mass abundance must therefore be re-scaled to the true value  $X'_j$  given by

$$X'_j = \frac{X_j}{\sum X_j} \quad (7)$$

Finally the *total enhancement factor*  $\Gamma$  is

$$\Gamma = -\log \left( \frac{X'_{Fe}}{X_{Fe}^{\odot}} \right) \quad (8)$$

from which we immediately get the relationship between  $\Gamma$  and the new value of the Fe abundance in  $\alpha$ -enhanced mixtures

$$\log \left( \frac{X'_{Fe}}{X'_H} \right) = -\Gamma + \log \left( \frac{X_{Fe}}{X_H} \right)_{\odot} + \log \left( \frac{X'}{X_H^{\odot}} \right) \quad (9)$$

The abundance ratios and total degree of enhancement for the case we are going to consider are listed in Table 2. The case with  $\Gamma=0.25$  corresponds to the  $\alpha$ -enhanced chemical compositions chosen by Munari et al. (2004) for their 1 Å resolution spectra.

Finally, it is worth calling attention that at given total metallicity  $Z$  different patterns of  $[X_j/X_{Fe}]$  may yield the same total enhancement factor  $\Gamma$ . This fact bears very much on the correction of indices for enhancement because each elemental species brings a different effect.

### 2.3 The Worthey et al. (1994) and Borges et al. (1995) Fitting Functions

The Lick  $\mathcal{FF}$ s refer to 25 absorption line indices (Worthey 1992; Worthey et al. 1994; Worthey & Ottaviani 1997) and are based on a library of stellar spectra containing about 400 stars, observed at the Lick Observatory between 1972 and 1984, with an Image Dissector Scanner (IDS). In the following we adopt the Worthey (1992)  $\mathcal{FF}$ s, extended however to high temperature stars ( $T_{\text{eff}} \approx 10000$  K) as reported in Longhetti et al. (1998). Recently new  $\mathcal{FF}$ s are available also for the  $\lambda 4000$  break by Gorgas et al. (1999) and Ca II triplet by Cenarro et al. (2001). All these  $\mathcal{FF}$ s depend on stellar effective temperature, gravity and metallicity ( $[\text{Fe}/\text{H}]$ ). They do not explicitly include the effect of  $\alpha$ -enhancement.

Many studies have emphasized that absorption line indices should also depend on the detailed pattern of chemical abundances (Barbuy 1994; Idiart & de Freitas-Pacheco 1995; Weiss et al. 1995; Borges et al. 1995), in particular when some elements are enhanced with respect to the solar value. Empirical  $\mathcal{FF}$ s for  $\text{Mg}_2$  and  $\text{NaD}$  in which the effect of enhancement is considered have been presented by Borges et al. (1995). For all other indices one has to use the Worthey (1992)  $\mathcal{FF}$ s, in which the effect of enhancement is missing, but for the re-scaling of  $[\text{Fe}/\text{H}]$  given by eqn. (9). A great deal of the effect of enhancing  $\alpha$ -elements is simply lost.

### 2.4 The Tripicco & Bell (1995) Response Functions

A general method designed to include the effects of enhancement on all indices at once has been suggested by Tripicco & Bell (1995, TB95), who introduce the concept of  $\mathcal{RF}$ s. In brief from model atmospheres and spectra for three prototype stars, i.e. a Cool-Dwarf star (CD) with  $T_{\text{eff}}=4575$  K and  $\log g=4.6$ , a Turn-Off (TO) star with  $T_{\text{eff}}=6200$  K and  $\log g=4.1$ , and a Cool-Giant (CG) star with  $T_{\text{eff}}=4255$  K and  $\log g=1.9$ , they calculate the reference indices  $I_0$  for the solar abundance ratios. Separately doubling the abundance  $X_i$  of the C, N, O, Mg, Fe, Ca, Na, Si, Cr, and Ti in steps of  $\Delta[\text{X}_i/\text{H}]=0.3$  dex, they determine the variation  $\Delta I = I_{\text{enh}} - I_0$  in units of the observational error  $\sigma_0$ . The indices  $I_0$ , the observational error  $\sigma_0$ , and the normalized  $\Delta I$  are given in Tables 4, 5 and 6 of TB95.

The definition of the generic  $\mathcal{RF}$  to be used for arbitrary variations  $\Delta[\text{X}_i/\text{H}]$  is

**Table 2.** Abundance ratios for the solar-scaled and  $\alpha$ -enhanced mixtures adopted in this study. The solar scaled values are taken from Anders & Grevesse (1989) however as revised by Grevesse & Sauval (1998). The enhancement factor  $[\text{X}_{\text{el}}/\text{Fe}] = +0.40$  is the same as in Castelli & Kurucz (2004).

Element	$\Gamma = 0$	$\Gamma = 0.25$			
		$A_{\text{el}}$	$A_{\text{el}}$	$\frac{X_{\text{el}}}{\text{Fe}}$	$\frac{X_{\text{el}}}{\text{H}}$
O	8.83	9.23	0.40	0.1490	
Ne	8.08	8.08	0.00	-0.2510	
Mg	7.58	7.98	0.40	0.1490	
Si	7.55	7.95	0.40	0.1490	
S	7.33	7.73	0.40	0.1490	
Ca	6.36	6.76	0.40	0.1490	
Ti	5.02	5.42	0.40	0.1490	
Ni	6.25	6.25	0.00	-0.2510	
C	8.52	8.52	0.00	-0.2510	
N	7.92	7.92	0.00	-0.2510	
Na	6.33	6.33	0.00	-0.2510	
Cr	5.67	5.67	0.00	-0.2510	
Fe	7.50	7.50	0.00	-0.2510	

$$R_{0.3}(i) = \frac{1}{I_0} \frac{\Delta I}{\Delta[\text{X}_i/\text{H}]} \cdot 0.3$$

The  $\mathcal{RF}$ s for Cool-Dwarfs, Cool-Giants, and Turn-Off stars constitute the milestones of the calibration. They are used by Trager et al. (2000b), Thomas et al. (2003a), and TC04a to transfer indices with solar abundance ratios to those enhanced in  $\alpha$ -elements by means of two different algorithms. Since they are not strictly equivalent, some clarification is worth here.

Without providing a formal justification, Trager et al. (2000b) propose that the fractional variation of an index to changes of the chemical parameters is the same as that for the reference index  $I_0$  according to the relation

$$\frac{\Delta I}{I} = \frac{\Delta I_0}{I_0} = \left\{ \prod_i [1 + R_{0.3}(i)]^{\frac{[\text{X}_i/\text{H}]}{0.3}} \right\} - 1 \quad (10)$$

where  $R_{0.3}(i)$  are the  $\mathcal{RF}$ s we have defined above. The explanation of relation (10) has been provided by TC04a to whom the reader should refer for details. The advantage with this formulation is that no particular constraint is required on the sign of  $I_0$ , and the  $\Delta I$  given by TB95 are straightforwardly used.

A different reasoning has been followed by Thomas et al. (2003a). In brief, they start from the observational hint that in Galactic stars  $\text{Mg}_2 \propto \exp([\text{Mg}/\text{H}])$  (see Borges et al. 1995), assume that all indices depend exponentially on the abundance ratios and introduce the variable  $\ln I \propto [\text{X}_i/\text{H}]$ , expand  $\ln I$  in the Taylor series, and by replacing the partial derivatives with respect to abundances by the finite incremental ratios of TB95, express the fractional variation of an index to changes in the abundance ratios as

$$\frac{\Delta I}{I} = \left\{ \prod_i \exp(R_{0.3}(i))^{\frac{[\text{X}_i/\text{H}]}{0.3}} \right\} - 1 \quad (11)$$

The reader is referred to Thomas et al. (2003a) for the formal derivation of relation (11). Although relations (10) and (11)

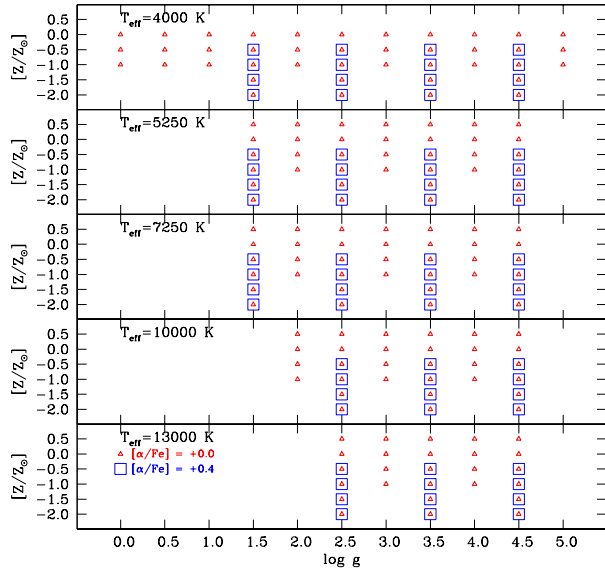


**Figure 1.** Coverage in the atmospheric parameters, and  $[\alpha/\text{Fe}]$  of the  $1\text{\AA}$  resolution spectra used in this study. The filled triangles are for chemical compositions with solar abundance ratios  $[\alpha/\text{Fe}] = 0$  and  $\Gamma = 0$ , whereas the open squares are  $\alpha$ -enhanced mixtures  $[\alpha/\text{Fe}] = +0.4$  and  $\Gamma = 0.25$

may look similar, actually they do not because in the latter the partial derivatives in the Taylor expansion have been replaced by the finite incremental ratios. This topic has been thoroughly discussed by TC04a.

The following remarks are worth to be made here. Firstly as emphasized by Trager et al. (2000b) and Thomas et al. (2003a), eqns. (10) and (11) while securing that the indices tend to zero for small abundances they let them increase with the exponent  $[X_i/\text{H}]/0.3$ . For abundances higher than  $[X_i/\text{H}] = +0.6$  dex, the exponent may became too large and consequently both types of correction may diverge. Secondly, the use of eqns. (10) and (11) requires that the sign of the index to be corrected is the same of the corresponding  $I_0$  in TB95. In general this holds good. In principle, it may, however, happen that the signs do not coincide. Furthermore, some of the indices  $I_0$  in TB95 are negative so that the  $\ln I$  variable cannot be defined and the Taylor expansions can no longer be applied. To overcome this potential difficulty, Thomas et al. (2003a) apply a correcting procedure forcing the negative reference indices  $I_0$  of TB95 to become positive. This occurs in particular for  $H_\beta$  of Cool-Dwarf stars (and other indices as well). The argument is that neglecting non-LTE effects TB95 underestimate the true values of  $H_\beta$  so that negative values found for temperatures lower than about 4500 K should be shifted to higher, positive values, see for instance Fig. 12 in TB95. We suspect that any change to the values tabulated by TB95 may be risky for a number of reasons: (i) The  $\mathcal{FF}$ s have been derived from a set of data that include a significant number of stars with negative values of  $H_\beta$ ; (ii) The incremental ratios by TB95 have been calculated for particular stars (stellar spectra) with assigned  $T_{\text{eff}}$ ,  $\log g$ , and  $I_0$ . Changing the reference  $I_0$  while leaving unchanged the incremental ratios (partial derivatives) may not be very safe; (iii) The replacement of the partial derivatives with the TB95 incremental ratios may

be risky when dealing with exponential functions; (iv) The corrections found by Thomas et al. (2003a) for a number of indices are quite large; (v) Finally, the use of  $\ln I$  as dependent variable which requires that only positive values for  $I_0$  are considered.

The application of eqns. (10) and (11) by TC04a has generated different and highly controversial results for some indices,  $H_\beta$  in particular, under unusual enhancements in some elements. In brief, TC04a presented grids of indices with  $\alpha$ -enhanced abundance ratios. The indices were derived from the Salasnich et al. (2000) stellar models and isochrones with the abundance ratios by Ryan et al. (1991), and corrected by means of eqn. (10) of Trager et al. (2000b). The unusual abundance ratio for Ti ( $[\text{Ti}/\text{Fe}] = 0.63$ ) together with the interpolation among the fractional variations of the calibrating stars, yielded  $H_\beta$  strongly increasing with  $\Gamma$ . This immediately reflected on the ages assigned to galaxies by means of the *Minimum-Distance Method* of Trager et al. (2000b,a) widely used by TC04a. The strong impact of Ti on  $H_\beta$  is due to the high  $\mathcal{RF}$  of this element for cool-dwarfs in the TB95 calibration. Decreasing the ratio  $[\text{Ti}/\text{Fe}]$  to zero as in Trager et al. (2000b) or to 0.3 as in Thomas et al. (2003a), the results by TC04a were in close agreement with those by the other authors. It is worth recalling that the ratio  $[\text{Ti}/\text{H}]$  entering eqns. (10) and (11), was 0 in Trager et al. (2000b), 0.023 in Thomas et al. (2003a), and nearly 0.2 in TC04a with obvious consequences. The effect was also confirmed by adopting the more recent determinations by Carney (1996) and Habgood (2001) of the  $[\text{Ti}/\text{Fe}]$  in globular clusters that yield  $\langle [\text{Ti}/\text{Fe}] \rangle \simeq 0.25 \div 0.30$ , and by Gratton et al. (2003) for a sample of metal-poor stars with accurate parallaxes for which they yields  $\langle [\text{Ti}/\text{Fe}] \rangle \simeq 0.20 \pm 0.05$  (TC04a). In any case the controversy about the correcting technique still remained. It can be reduced to the following statement: does  $H_\beta$  increase (significantly) with  $\Gamma$  or not? Or, even worse, does it decrease with it? According to Thomas et al. (2003a) there should be no difference in  $H_\beta$  at increasing  $\Gamma$ . The analysis below will clarify that this is not the case.

### 3 THE NEW RESPONSE FUNCTIONS

The above procedure for calculating indices and including  $\alpha$ -enhancement will become obsolete when theoretical high resolution spectra for different values of gravity, effective temperature, metallicity and degree of enhancement are available. In such a case, indeed, the indices can be straightforwardly calculated from the spectra with no need of the  $\mathcal{FF}$ s and the  $\mathcal{RF}$ s.

#### 3.1 The high resolution spectra

The spectra used in the present analysis are taken for a partial pre-release of the  $2500\text{--}10500\text{\AA}$  extensive synthetic spectral library computed by Munari et al. (2004). The spectral library is based on the new grid of ATLAS9 model atmospheres computed by Castelli & Kurucz (2004) for new opacity distribution functions that include, among other characteristics, the replacement of the solar abundances by Anders & Grevesse (1989) with those from Grevesse & Sauval (1998), and the TiO line-list by Kurucz

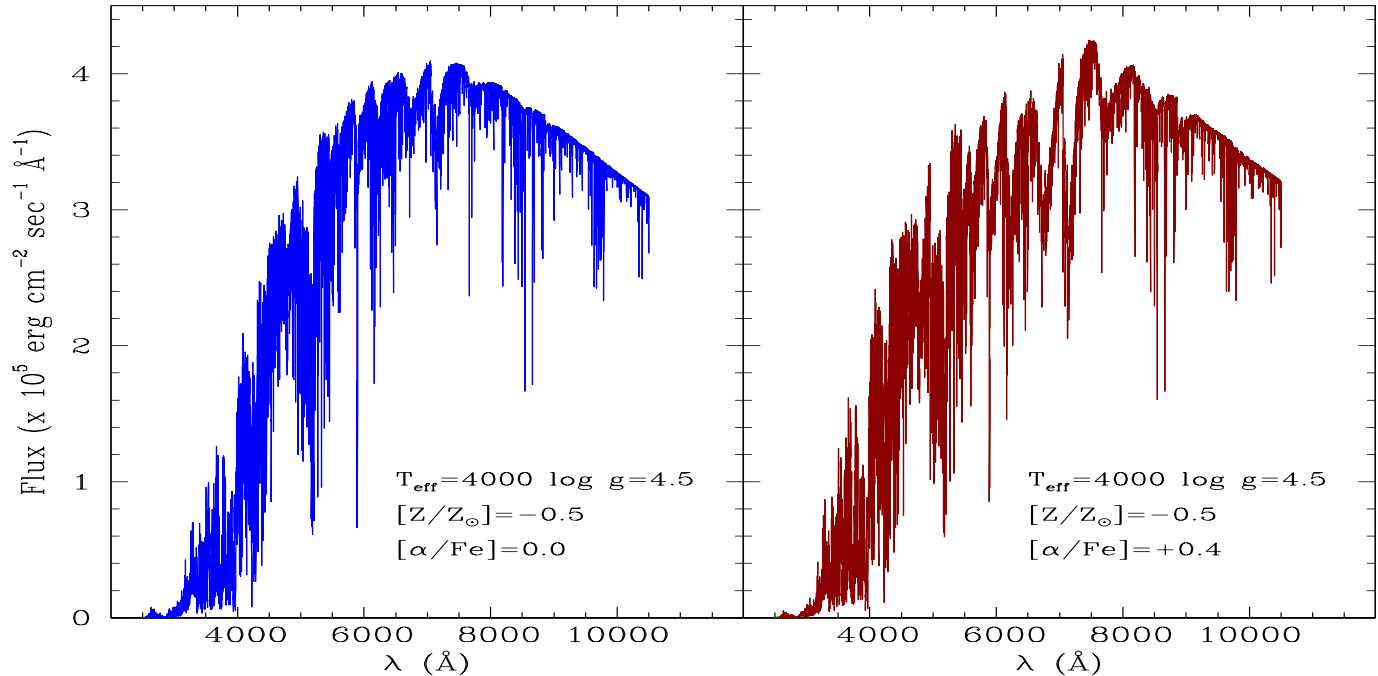


**Figure 2.** Left: Spectral energy distribution  $F_\lambda$  for the star with  $T_{\text{eff}}=4000$  K,  $\log g=4.5$ ,  $[\text{Z}/\text{Z}_\odot]=-0.5$ ,  $[\alpha/\text{Fe}]=0.0$  and  $\Gamma=0$ . The wavelength is in  $\text{\AA}$ .  $F_\lambda$  is in  $\text{erg sec}^{-1}\text{cm}^{-2}\text{\AA}^{-1}$  and the resolution is  $1\text{\AA}$ . Right: the same but for  $[\alpha/\text{Fe}]=+0.4$  and  $\Gamma=0.25$

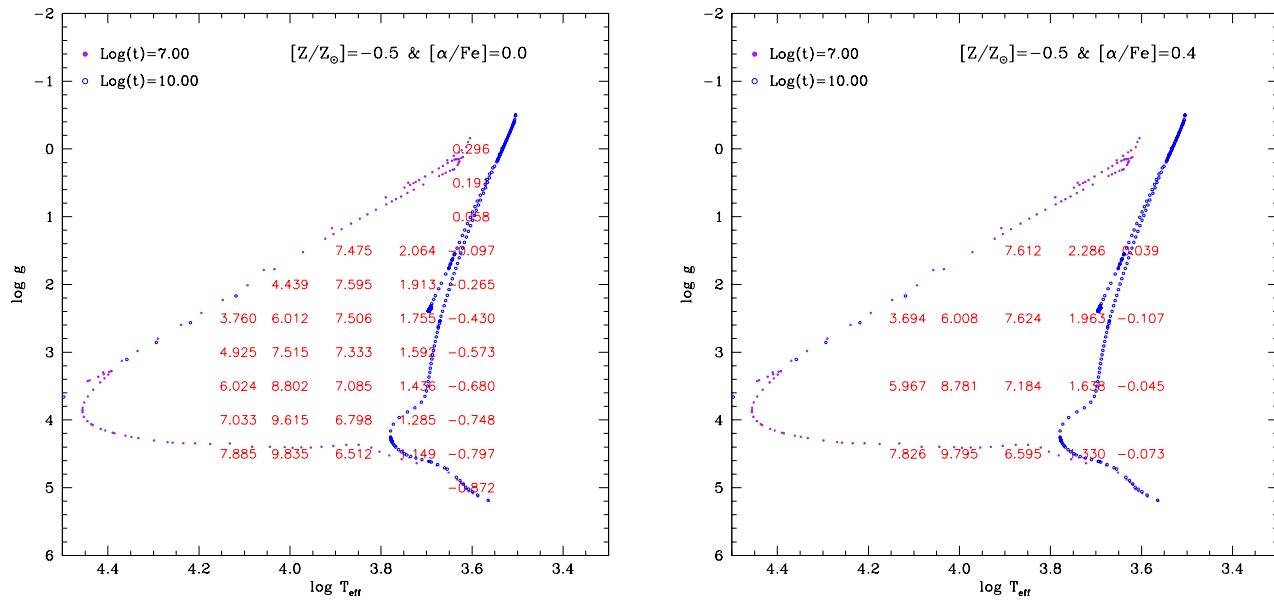


**Figure 3.** Variation of  $H_\beta$  from  $1\text{\AA}$  resolution spectra across the HR-Diagram in the  $\log g$  vs.  $\log T_{\text{eff}}$  plane. Each value of  $H_\beta$  corresponds to a star (theoretical spectrum) of given  $\log g$ ,  $T_{\text{eff}}$ , and  $[\text{Z}/\text{Z}_\odot]$ . The case under consideration is for  $[\text{Z}/\text{Z}_\odot]=-0.5$  and  $[\alpha/\text{Fe}]=0.0$ . In the same diagrams we also plot two isochrones of the Padova Library with the same metallicity ( $Z=0.008$ ) and ages of 0.01 and 10 Gyr.

(1993) with that of Schwenke (1998). The Munari et al. (2004) spectral library includes more than 200,000 spectra at resolutions of 20,000 and 2000 (the latter matching the SLOAN spectra), as well as uniform dispersions of  $1\text{\AA}/\text{pix}$  and  $10\text{\AA}/\text{pix}$ . In this work we have made use of the library version at  $1\text{\AA}/\text{pix}$ . The spectra cover the tempera-

ture range  $3500\text{--}50000$  K, gravity  $0.0\leq\log g\leq5.0$ , metallicities  $-2.5\leq[\text{Z}/\text{Z}_\odot]\leq+0.5$ , micro-turbulence velocities  $0, 1, 2, 4$   $\text{km/sec}$ , enhancements  $[\alpha/\text{Fe}]=0.0, +0.4$  and a dozen of different rotational velocities. When completed, the whole library will be used for a more complete analysis of the Lick indices and their applications. A strictly coordinated library

of synthetic spectra is the one published by Zwitter et al. (2004) for the GAIA and RAVE wavelength range, amounting to 183,588 spectra covering a similar space of parameters.

The temperature, gravity and metallicity coverage of the stellar spectra in usage here is summarized in Fig. 1. Each panel is for a different effective temperature as indicated. The symbols show the combination of metallicity, expressed here in spectroscopic notation as  $[Z/Z_\odot] = \log(Z/Z_\odot)$ , and gravity ( $\log g$ ) for which a spectrum has been calculated. The triangles are for  $[\alpha/\text{Fe}] = 0.0$  whereas the squares are for  $[\alpha/\text{Fe}] = +0.4$ . The parameters span the following ranges: two values of  $[\alpha/\text{Fe}]$ , i.e.  $[\alpha/\text{Fe}] = 0.0$  and  $+0.4$ ; six values of  $[Z/Z_\odot]$  i.e.  $-2.0, -1.5, -1.0, -0.5, 0.0$  and  $0.5$ ; five values of  $T_{\text{eff}}$ , i.e.  $4000, 5250, 7250, 10000$ , and  $13000$  K; and finally eleven values of  $\log g$  going from  $0.0$  to  $5.0$  in steps  $0.5$ . The spectral grid is only a sub-set of the original model atmosphere grid, however fully adequate to the purposes of this study. The range of wavelength in each spectrum goes from  $2500 \text{ \AA}$  to  $10500 \text{ \AA}$  with resolution of  $1 \text{ \AA}$ . The flux  $F_\lambda$  is in  $\text{erg sec}^{-1} \text{cm}^{-2} \text{\AA}^{-1}$ . In Fig. 2 we show for the sake of illustration the spectral energy distribution for the model with  $T_{\text{eff}} = 4000$  K,  $\log g = 4.5$ ,  $[Z/Z_\odot] = -0.5$ , micro-turbulence velocity  $k = 2 \text{ km/sec}$ , and  $[\alpha/\text{Fe}] = 0.0$  (left panel) and  $+0.4$  (right panel). This model fairly represents the case of a cool-dwarf star.

### 3.2 Indices from 1 Å resolution spectra

With the aid of eqns. (1) and/or (2) and the pass-bands of Trager et al. (1998) listed in Table 1 we filter the energy distribution of each star in our grids, and derive the indices on the Lick system. The data for the whole sets of indices are not displayed but they are partly given in and partly recovered from Tables A1 through A4 to be described in Appendix. We limit ourselves to show in Fig. 3 and Fig. 4 the variation of the index  $H_\beta$  across the HR-Diagram for the case with  $[Z/Z_\odot] = -0.5$  and  $[\alpha/\text{Fe}] = 0.0$  and  $+0.4$ . In the same diagram we also plot two isochrones with the same metal content taken from the Padova Library (Girardi 2003, private communication): the ages are  $0.01 \text{ Gyr}$  and  $10 \text{ Gyr}$ . The grids of calibrating stars cover most of the HR-diagram in which real stars are found.

### 3.3 New Response Functions

It is worth of interest here to present the analogue of the TB95  $\mathcal{RF}$ s, the only major difference is that they cannot be evaluated for separate increases in the abundance of individual species  $[\alpha_i/\text{Fe}]$  but only for all elements enhanced with respect to the solar value lumped together. Now the dependence of the  $\mathcal{RF}$ s on temperature, gravity, metallicity, and enhancement can be evaluated in detail. This was not the case with TB95 calibration which stood on three stars with solar metallicity. We start calculating the differences

$$(\delta I)_{T_{\text{eff}}, \log g, [Z/Z_\odot]} = I_{\text{enh}} - I_{\text{sol}} \quad (12)$$

taken at fixed  $T_{\text{eff}}$ ,  $\log g$ , and metallicity ( $[Z/Z_\odot]$ ) and varying  $[\alpha/\text{Fe}]$  from  $0.0$  to  $+0.4$ , whose corresponding indices are indicated as  $I_{\text{sol}}$  and  $I_{\text{enh}}$ , respectively. The difference

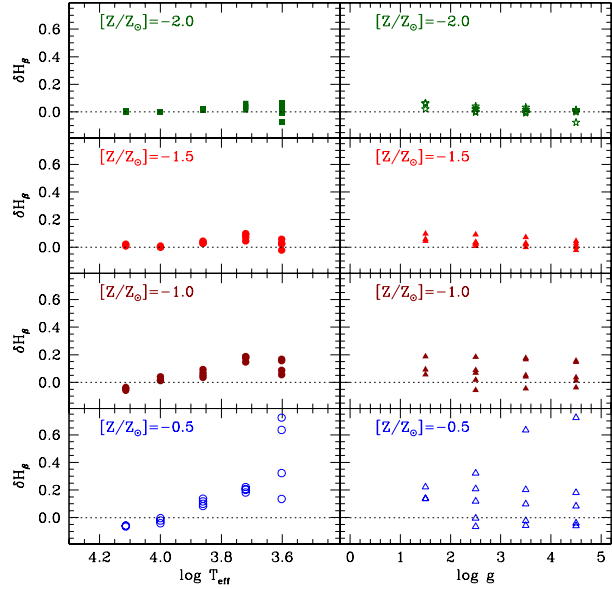


**Figure 5.** Variations of the index  $H_\beta$  passing from solar to  $\alpha$ -enhanced chemical mixture. We plot the difference  $(\delta I)_{T_{\text{eff}}, \log g, [Z/Z_\odot]}$  as a function of the atmospheric parameters as indicated. Left panels: for each  $T_{\text{eff}}$   $\delta H_\beta$  increases with  $\log g$ . Right Panels: for each  $\log g$   $\delta H_\beta$  decreases with  $T_{\text{eff}}$ .

for the whole sets of values are given in Tables A1, A2, A3, and A4 for  $[Z/Z_\odot] = -2.0$ ,  $[Z/Z_\odot] = -1.5$ ,  $[Z/Z_\odot] = -1.0$ , and  $[Z/Z_\odot] = -0.5$ , respectively.

In the four panels of Fig. 5 we show the case of  $H_\beta$ . Each panel displays the variation of  $H_\beta$  at changing  $T_{\text{eff}}$  and/or  $\log g$ . We note that, for any metallicity and passing from  $[\alpha/\text{Fe}] = 0.0$  to  $+0.4$ : (i) at given  $T_{\text{eff}}$   $\delta H_\beta$  increases at increasing  $\log g$ ; (ii) at given  $\log g$   $\delta H_\beta$  increases at decreasing  $T_{\text{eff}}$ . For most cases  $\delta H_\beta$  is positive, i.e. the *index  $H_\beta$  increases at increasing  $[\alpha/\text{Fe}]$*  or, in other words,  $H_\beta$  for  $\alpha$ -enhanced mixtures is greater than the solar case, keeping all other parameters constant. The increase is always significant, say about  $0.1 \div 0.2$ , but it can amount to nearly  $0.8$  for stars of low  $T_{\text{eff}}$  and high gravity, roughly in the intervals covered by cool-dwarf and old turn-off stars, which are the most interesting in view of the forthcoming applications.

Why such an increase with  $\alpha$ ? The answer lies in relative variation of  $F_l$  and  $F_c$ . In the case of  $H_\beta$  (our prototype index) we derive the variation  $(\delta I)$  passing from solar to  $\alpha$ -enhanced mixtures. Upon differentiating the index with respect to  $F_l$  and  $F_c$  ( $\frac{\partial I}{\partial F_l} = -\frac{1}{F_c} \Delta \lambda$  and  $\frac{\partial I}{\partial F_c} = \frac{F_l}{F_c^2} \Delta \lambda$ ) we get

$$(\delta I) = \Delta \lambda \left( \frac{F_l}{F_c} \right)_{\text{sol}} [\Delta \ln F_c - \Delta \ln F_l] \quad (13)$$

where  $\Delta \ln F_l$  and  $\Delta \ln F_c$  are the differences in the line and continuum fluxes passing from enhanced to solar. Plugging the values of  $F_l$  and  $F_c$  as appropriate, it turns out that the index increases with  $\alpha$ . What happens is best illustrated in Fig. 6 which, limited to the case of a typical Cool-Dwarf with  $T_{\text{eff}} = 4000$ ,  $\log g = 4.5$ , and  $[Z/Z_\odot] = -0.5$  ( $Z = 0.008$ ), shows how the index  $H_\beta$  is built up and how it varies passing from  $[\alpha/\text{Fe}] = 0.0$  to  $[\alpha/\text{Fe}] = +0.4$ . Firstly in the bottom panel we display the ratio  $F_{\lambda, \text{enh}}/F_{\lambda, \odot}$  and the pass-bands defining the index  $H_\beta$ . The absorption in the  $\alpha$ -enhanced spectrum

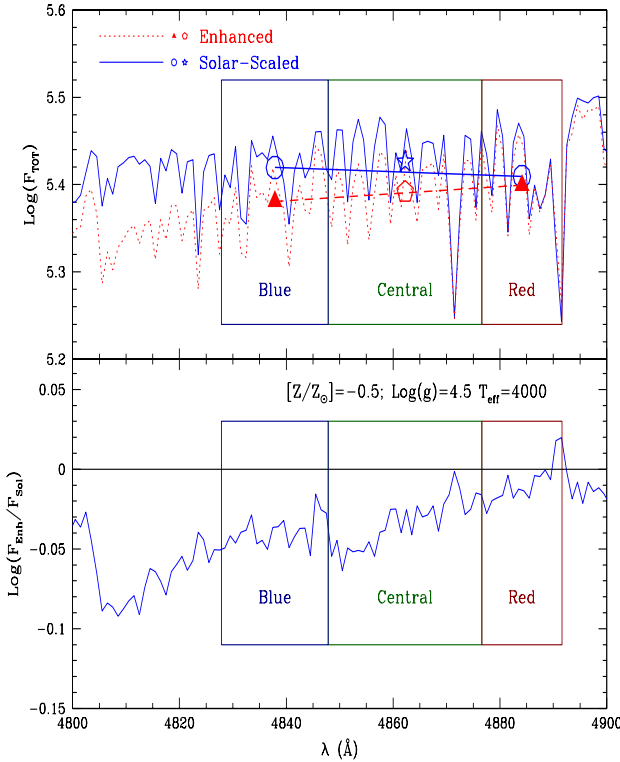


**Figure 6.** Building-up of the index  $H_\beta$  in the cool dwarf with  $T_{\text{eff}}=4000$ ,  $\log g=4.5$ , and  $[Z/Z_\odot]=-0.5$  both for the solar scaled and enhanced pattern of abundance ratios with  $[\alpha/\text{Fe}]=+0.4$ . The bottom panel shows the ratio  $F_{\lambda, \text{enh}}/F_{\lambda, \odot}$ . The absorption in the  $\alpha$ -enhanced spectrum is significantly larger than the solar-scaled one. The effect is larger in the blue wing of the pseudo-continuum and central band than in the red pseudo-continuum. Upper panel the spectral energy distribution of the solar-scaled (solid line) and  $\alpha$ -enhanced (dotted line) spectrum and the passbands defining the index  $H_\beta$ . The open circles and star show the mean fluxes in the three pass-band and the interpolation of the pseudo-continuum to derive  $F_c$  in the case of solar scaled spectrum. The filled triangles and pentagon are the same but for the  $\alpha$ -enhanced mixture. The increase of  $H_\beta$  passing from solar to  $\alpha$ -enhanced abundance ratios is straightforward.

is significantly larger than in the solar-scaled one. The effect is larger in the blue pseudo-continuum and central band than in the red pseudo-continuum. This means that  $\alpha$ -enhanced mixtures distort the spectrum in such a way that simple predictions cannot be made. This is due to the contribution of hundreds of molecular and atomic lines falling into the spectral regions over which the index is defined. Secondly, in the upper panel we show the spectral energy distribution of the solar-scaled (solid line) and  $\alpha$ -enhanced (dotted line) spectrum and once more the pass-bands for  $H_\beta$ . The open circles and the big empty star show the mean fluxes in the three pass-bands and the interpolation of the pseudo-continuum to derive  $F_c$  in the case of solar scaled spectrum. The filled triangles and the empty pentagon are the same but for the  $\alpha$ -enhanced mixture. The increase of  $H_\beta$  passing from solar to  $\alpha$ -enhanced abundance ratios is straightforward.

With the differences  $(\delta I)$ , the equivalent of the TB95  $\mathcal{RF}$ s  $R_{0.3}(X_i)$ s

$$R_{0.4}(\alpha) = \frac{1}{I_{\text{sol}}} \frac{I_{\text{enh}} - I_{\text{sol}}}{\Delta[\alpha/\text{Fe}]} 0.4 \quad (14)$$

where the symbol  $\alpha$  reminds the reader that only variation for all elements enhanced at a time are available (the products in eqns. (10) and (11) would extend over one term only). Work is in progress to exactly repeat the analysis made by TB95, i.e. to provide partial  $\mathcal{RF}$ s by separately enhancing individual elements at a time. This would improve upon the  $\mathcal{RF}$ s and yet maintain alive the  $\mathcal{FF}$ s until high resolution spectra will become a general tool.

Having done that, for the sake of a preliminary investigation of the whole subject, we extrapolate the results obtained for  $[Z/Z_\odot]=-2.0, -1.5, -1.0$ , and  $-0.5$  to higher values of the metallicity, i.e.  $[Z/Z_\odot]=0$  and  $0.5$ . The extrapolation is safe, thanks to the linear dependencies of the quantity  $(\delta I)=I_{\text{enh}}-I_{\text{sol}}$  on the atmospheric parameters (already shown in Fig. 5).

#### 4 SSP INDICES FROM $\mathcal{FF}$ s AND NEW $\mathcal{RF}$ s

Owing to the large body of data and synthetic indices on the Lick system, it might be worth of interest to derive indices still based on the  $\mathcal{FF}$ s but in which the old  $\mathcal{RF}$ s are replaced by the new ones. This means that indices for the case  $[\alpha/\text{Fe}]=0.0$  are calculated as amply described in TC04a, whereas those for  $[\alpha/\text{Fe}]>0.0$  are obtained according to the following equation

$$I_{i, \text{enh}} = I_{i, \text{sol}} + \delta \mathcal{I}_i \quad (15)$$

where  $I_{i, \text{sol}}$  is the solar-scaled index of the generic star in the SSP, and  $I_{i, \text{enh}}$  is the same but corrected for enhancement by  $\delta \mathcal{I}_i$ . This is derived by linearly interpolating both in  $\log g$  and  $T_{\text{eff}}$  the new  $\mathcal{RF}$ s (listed in Tables A1, A2, A3, and A4)<sup>2</sup>.

##### 4.1 Definition

The integrated indices of SSPs can be derived in the following way. We start from the flux in the absorption line of the generic star of the SSP,  $F_{l, i}$ <sup>3</sup>

$$F_{l, i} = F_{c, i} \left( 1 - \frac{I_{l, i}}{\Delta_\lambda} \right) \quad (16)$$

where  $I_{l, i}$  is the index derived from the  $\mathcal{FF}$ s using the  $T_{\text{eff}}$ ,  $\log g$ , and chemical composition of the star, and in the case of  $\alpha$ -enhancement also corrected according to eqn. (15).  $F_{c, i}$  is the pseudo-continuum flux, and  $F_{l, i}$  is the flux in the pass band. The flux  $F_{c, i}$  is calculated by interpolating to the central wavelength of the absorption line, the fluxes in the midpoints of the red and blue pseudo-continua bracketing the line (Worley et al. 1994).

<sup>2</sup> It is worth recalling that an equivalent procedure would be to use eqn. (10) combined with (14) instead of eqn. (15)

<sup>3</sup> The relation for indices measured in magnitudes is

$$F_{l, i} = F_{c, i} 10^{-0.4 I_{l, i}}$$

**Table 3.** Chemical composition and [Fe/H] as function of  $\Gamma$  for the SSPs in use.

Z	Y	X	$\Gamma = 0.0$	$\Gamma = 0.25$
			[Fe/H]	[Fe/H]
0.008	0.248	0.7440	-0.3972	-0.6472
0.019	0.273	0.7080	0.0000	-0.2501
0.040	0.320	0.6400	0.3672	0.1172
0.070	0.338	0.5430	0.6824	0.4324

To calculate the flux  $F_{c,i}$  of a generic star one needs the theoretical spectrum of the same star. To be able to compare our results based on the  $\mathcal{RF}$ s with old ones by (Trager et al. (2000b); Thomas et al. (2003a), and TC04a) based on low resolution spectra, we have to make use of stellar spectra with similar resolution. Therefore we leave aside the library of high resolution spectra of Munari et al. (2004) and adopt the low resolution one amalgamated by Girardi et al. (2002) and adopted by TC04a. Since the backbone of this library are the Kurucz ATLAS9 model atmospheres and stellar spectra, there is partial consistency between the spectra adopted to evaluate the pseudo-continuum and the 1 Å resolution spectra adopted to derive the new  $\mathcal{RF}$ s.

Known the fluxes  $F_{l,i}$  and  $F_{c,i}$  for a single star, we weigh its contribution to the integrated value on the relative number of stars of the same type. Therefore the integrated index is given by

$$I_l^{SSP} = \Delta_\lambda \left( 1 - \frac{\sum_i F_{l,i} N_i}{\sum_i F_{c,i} N_i} \right) \quad (17)$$

where  $N_i$  is the number of stars in the bin<sup>4</sup>.

When computing actual SSPs, single stars are identified to the isochrone elemental bins defined in such a way that all relevant quantities, i.e. luminosity,  $T_{\text{eff}}$ ,  $\log g$ , and mass vary by small amounts. In particular, the number of stars in an isochrone bin is given by

$$N_i = \int_{m_a}^{m_b} \phi(m) dm \quad (18)$$

where  $m_a$  and  $m_b$  are the minimum and maximum star mass in the bin and  $\phi(m)$  is the mass function in number. These are the equations adopted to calculate the indices of SSPs.

Finally, in view of the discussion below it is worth reminding the reader the definition of two indices that are commonly used but which do not belong to the original Lick system. They are  $\langle \text{Fe} \rangle$  and  $[\text{MgFe}]$

$$\langle \text{Fe} \rangle = 0.5 \times (Fe5270 + Fe5335)$$

$$[\text{MgFe}] = \sqrt{\text{Mg}_b \times (0.5 \times Fe5270 + 0.5 \times Fe5335)}$$

<sup>4</sup> The same expression for indices measured in magnitudes becomes

$$I_l^{SSP} = -2.5 \log \left( \frac{\sum_i F_{l,i} N_i}{\sum_i F_{c,i} N_i} \right)$$

## 4.2 Stellar models and isochrones

For the purposes of this study, we adopt the Padova Library of stellar models and companion isochrones according to the release by Girardi et al. (2000) and Girardi (2003, private communication). This particular set of stellar models/isochrones differs from the classical one by Bertelli et al. (1994) for the efficiency of convective overshooting and the prescription for the mass-loss rate along the Asymptotic Red Giant Branch (AGB) phase. The stellar models extend from the ZAMS up to either the start of the thermally pulsing AGB phase (TP-AGB) or carbon ignition. No details on the stellar models are given here; they can be found in Girardi et al. (2000) and Girardi et al. (2002). Suffice it to mention that: (i) in low mass stars passing from the tip of red giant branch (T-RGB) to the HB or clump, mass-loss by stellar winds is included according to the Reimers (1975) rate with  $\eta=0.45$ ; (ii) the whole TP-AGB phase is included in the isochrones with ages older than 0.1 Gyr according to the algorithm of Girardi & Bertelli (1998) and the mass-loss rate of Vassiliadis & Wood (1993); (iii) four chemical compositions are considered as listed in Table 3.

## 4.3 Results for SSP indices

Going into a detailed description of the dependence of the absorption line indices for SSPs on age, chemical composition, and  $\Gamma$ , is beyond the scope of this study<sup>5</sup>. Suffice it to show in Fig. 7 the temporal evolution of eight important indices, i.e.  $\text{Mg}_b$ ,  $\text{Mg}_2$ ,  $H_\beta$ ,  $\langle \text{Fe} \rangle$ ,  $H_{\gamma\text{F}}$ ,  $H_{\delta\text{F}}$ ,  $[\text{MgFe}]$ , and  $C_{24668}$ , for the following combinations of metallicity and  $\Gamma$ , namely  $Z=0.008$  (solid lines) and  $Z=0.070$  (broken lines),  $\Gamma=0$  (heavy lines) and  $\Gamma=0.25$  (light lines). The age goes from 0.01 Gyr to 20 Gyr. These results are very similar to those found by TC04a adopting the same library of stellar spectra, the Worthey et al. (1994)  $\mathcal{FF}$ s, the old  $\mathcal{RF}$ s of TB95, and the algorithm of Trager et al. (2000b).

The two indices diagnostic planes are often used to infer the age, metallicity and degree of  $\alpha$ -enhancement, see TC04a for a thorough discussion of the subject. The most popular one is the  $H_\beta$  vs.  $[\text{MgFe}]$  plane shown in Fig. 8 which displays the whole range of values that are expected for the indices in question at varying metallicity (heavy solid lines), age (dotted lines), and  $\Gamma$  (hatched areas as indicated). Each hatched area is enclosed between the two SSPs with the lowest and highest metallicity in our sample, i.e.  $Z=0.008$  (left) and  $Z=0.070$  (right) and two lines of constant age (13 Gyr bottom and 2 Gyr top). Along each SSP four values of the age are marked, so that other lines of constant age can be drawn. The hatched areas are for  $\Gamma=0$  and  $\Gamma=0.25$  as indicated. The indices for the highest metallicity have been obtained using  $(\delta I)$  extrapolated to higher values of  $[\text{Z}/\text{Z}_\odot]$  (see Section 3.3). It is soon evident that models with the same  $Z$  and age may have significantly different  $H_\beta$  and  $[\text{MgFe}]$ . The same may occur for other pairs of indices in other diagnostic planes. The effect of  $\Gamma$  on  $H_\beta$  in particular, is far from being negligible as claimed in previous studies. Other values of  $\Gamma$  cannot be investigated at the present

<sup>5</sup> The complete grids of absorption line indices can be found on the web site <http://dipastro.pd.astro.it/galadriel>.

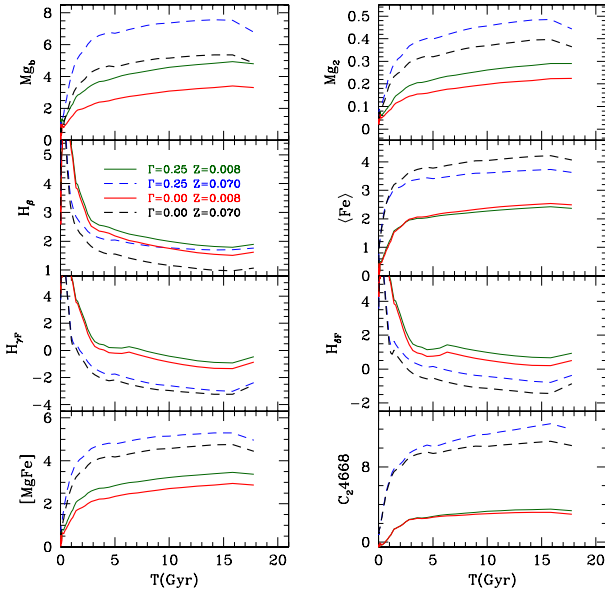


Figure 7. The temporal variation of different indices.

time for we simply lack the calibration (extrapolations to higher values of  $\Gamma$  cannot be safe). However, even with the present results we may predict that there is natural scatter in the diagnostic planes yielded by the degree of enhancement for which large ranges of values are possible depending on the particular star formation history of a galaxy (Tantalo & Chiosi 2004b). We will come back to this point later on in course of this study.

Since these indices are derived from the old  $\mathcal{FF}$ s on the Lick spectral library, they can be compared with the observational data for nearby galaxies based on spectra with similar resolution. The data are taken from the catalogs of Trager et al. (1998) –it includes the galaxies by González (1993)– for normal galaxies, and Longhetti et al. (2000) for shell- and pair-galaxies in which sign of dynamical interactions are present. The comparison is shown in Fig. 8 where the open triangles are the Trager et al. (1998) galaxies and the filled squares those by Longhetti et al. (2000).

#### 4.4 Passing from old to new $\mathcal{RF}$ s

In this section we compare indices derived from adopting the  $\mathcal{FF}$ s of Worthey et al. (1994) and the old  $\mathcal{RF}$ s of TB95 with those calculated here with the same  $\mathcal{FF}$ s but the new  $\mathcal{RF}$ s. They are shortly indicated as  $I_{\mathcal{ORF}}$ s and  $I_{\mathcal{NRF}}$ s, respectively. The indices  $I_{\mathcal{ORF}}$ s are taken from the extensive tabulations presented by TC04a. For the sake of brevity, the discussion is limited to four indices, namely  $H_\beta$ ,  $Mg_b$ ,  $\langle Fe \rangle$ , and  $Mg_2$  with  $Z=0.008$ . The correlation between  $I_{\mathcal{ORF}}$ s and  $I_{\mathcal{NRF}}$ s is shown in Fig. 9. The agreement is remarkably good. What we learn from this comparison is that

- i)  $\mathcal{FF}$ s and  $\mathcal{RF}$ s yield the gross dependencies of the indices on metallicity, age, and enhancement.
- ii) The new  $\mathcal{RF}$ s take into account effects that would otherwise be missed, in particular their dependence on the

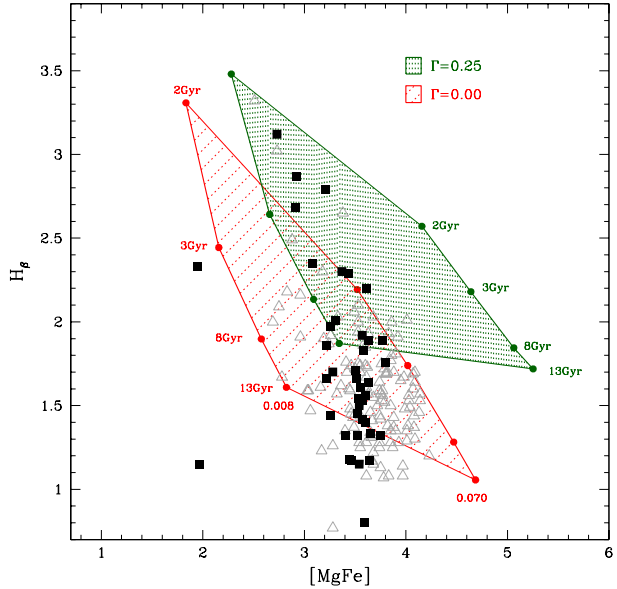


Figure 8.  $H_\beta$  vs.  $[MgFe]$  plane. Comparison between theory and observational data for galaxies in the Local Universe. Each hatched area is comprised between two SSP of different metallicity ( $Z=0.008$  left and  $Z=0.070$  right). Along each SSP the age increases from 2 Gyr (top) to 13 Gyr (bottom) and two more values of the age are marked (3 and 8 Gyr). Two lines of constant age are displayed, i.e. 2 and 13 Gyr. Each area is for a different  $\Gamma$ . The data for normal galaxies (open triangles) of Trager et al. (1998) and interacting galaxies (filled squares) of Longhetti et al. (2000).

metallicity.

- iii) The new  $\mathcal{RF}$ s for some indices and some stars, e.g.  $H_\beta$  for cool dwarfs, have the opposite dependence on  $[\alpha/Fe]$  as compared to that predicted by TB95. The result stems from the modern physical input of the new 1 Å resolution spectra. Furthermore it confirms that the method adopted by TC04a to correct for  $\alpha$ -enhancement was appropriate and physically sounded.
- iv) Looking at the correlations displayed in Fig. 9 while for  $H_\beta$  and  $Mg_b$  there is one-to-one correspondence,  $\langle Fe \rangle_{\mathcal{NRF}}$ s is systematically larger than  $\langle Fe \rangle_{\mathcal{ORF}}$ s by 0.3 Å, whereas  $Mg_2_{\mathcal{NRF}}$ s gets larger than  $Mg_2_{\mathcal{ORF}}$ s, roughly from 3% up to 33% at increasing age.

#### 4.5 Comparison with Galactic Globular Clusters

Before concluding this section, it is worth checking whether the present indices can reproduce the data for the Galactic Globular Clusters and Bulge by Puzia et al. (2002). To this aim we have taken the isochrones of the Padova Library with chemical composition typical of the Galactic Globular Clusters (Girardi et al. 2000), and derived the indices using the classical  $\mathcal{FF}$ s and the new  $\mathcal{RF}$ s. The results are shown in Fig. 10 for a number of indices. Along each line, are shown the indices of SSPs with same age but different metallicity from  $[Z/Z_\odot]=-2.0$  ( $Z \sim 0.0001$ ) to  $[Z/Z_\odot]=0.0$  ( $Z \sim 0.019$ ). The *thin solid* lines are the models with solar-scaled pattern of abundances, whereas the *thick-solid* are the models with

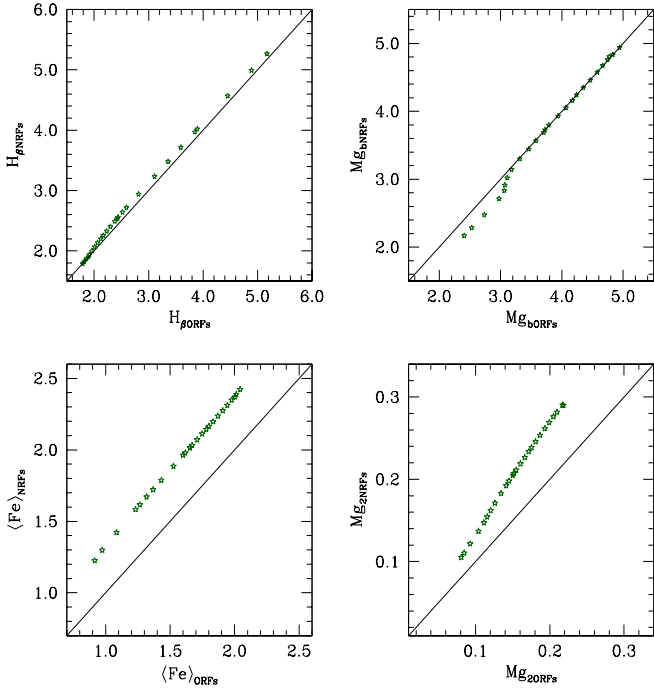


**Figure 9.** Comparison between  $H_\beta$  (top-left panel),  $Mg_b$  (top-right panel),  $\langle Fe \rangle$  (bottom-left panel), and  $Mg_2$  (bottom-right panel) calculated with the  $\mathcal{FF}$ s of Worthey et al. (1994) but different  $\mathcal{RFF}$ s, namely the old ones by TB95 and the new ones calculated here from the 1 Å resolution spectra. They are shortly indicated as  $I_{ORFFs}$  and  $I_{NRFs}$ , respectively. The comparison is limited to the metallicity is  $Z=0.008$  and  $\Gamma=0.25$ .

$\Gamma=0.25$  and/or  $[\alpha/Fe]=+0.4$ . Despite the fact that these indices were not particularly designed to match the Globular Clusters, the overall agreement is satisfactory. The new indices are of the same quality as those in TC04a and Thomas et al. (2003a). In general, the agreement is better for the solar-scaled mixture even though values of  $\Gamma$  in the range from 0.0 to 0.3 cannot be excluded. The index NaD depart from the observational value both in Thomas et al. (2003a), TC04a, and here.

## 5 SSPs INDICES MEASURED ON 1 Å RESOLUTION SPECTRA

In so far the key result of this study are the new  $\mathcal{RFF}$ s derived for a wider range of the atmospheric parameters and metallicities with respect to TB95. Even if this is a significant step forward, indices on the Lick system (or another system in general) can be directly obtained from high resolution spectra without passing through the  $\mathcal{FF}$ s and  $\mathcal{RFF}$ s, but simply filtering the spectral energy distribution of a star and/or SSP and/or galaxy. The only requirement to keep in mind is that the theoretical and observational spectra on which indices are measured, must have the same resolution. In this section we present for the first time indices on the Lick system directly measured on synthetic 1 Å resolution spectra.

Firstly we derive the theoretical indices for single stars of assigned atmospheric parameters, and compare them those for the stars in STELIB by Le Borgne et al. (2003)

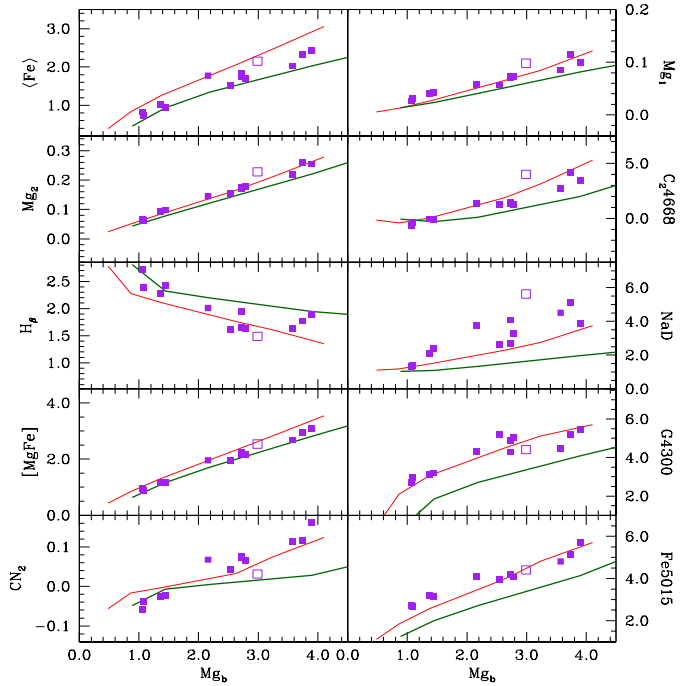


**Figure 10.** The index  $Mg_b$  index versus ten different indices on the Lick system calculated with metallicities typical of Globular Clusters. The *thin solid* lines are the models with solar-scaled pattern of abundances, whereas the *thick-solid* are the models with  $\Gamma=0.25$  and/or  $[\alpha/Fe]=+0.4$ . Along each line are shown the indices of SSPs with the same age, 12 Gyr and different metallicity from  $[Z/Z_\odot]=-2$  ( $Z \sim 0.0001$ ) to  $[Z/Z_\odot]=0.0$  ( $Z \sim 0.019$ ) These models are calculated with the classical  $\mathcal{FF}$ s and the new  $\mathcal{RFF}$ s. The filled squares are the globular cluster data, the open square is the Galactic Bulge from Puzia et al. (2002).

containing spectra at  $\sim 3$  Å resolution. Owing to the small difference in resolution between STELIB and Munari et al. (2004) spectra, we may reasonably surmise that the empirical indices of STELIB do not significantly differ from those obtained from the 1 Å spectra. Secondly, we analyse the behaviour of the new high-resolution indices in the same fashion as done in Section 4.3.

## 5.1 Indices for single stars and comparison with STELIB

The first step to undertake is to derive indices for a template of stars and compare them with the theoretical counterparts obtained from our library of 1 Å resolution spectra. To this aim we sort out from STELIB (Le Borgne et al. 2003) all stars with known  $T_{\text{eff}}$ ,  $\log g$ , metallicity and, more relevant here, complete spectra. About 141 stars meet the four requirements. Each star of our library is then associated to a star of the STELIB sub-sample by means of the minimum distance method in the space  $T_{\text{eff}}$ ,  $\log g$ , and  $[\text{Fe}/\text{H}]$  (or  $[Z/Z_\odot]$ ). Only theoretical spectra of the solar partition case ( $\Gamma=0$ ) are considered. The empirical and theoretical spectra of the selected sample are finally filtered with the Lick system and their indices are derived.

In Fig. 11 we show for each index the correspondence between the empirical (small dots) and the theoretical spectra (open circles) as a function of  $\log T_{\text{eff}}$ . Considering the

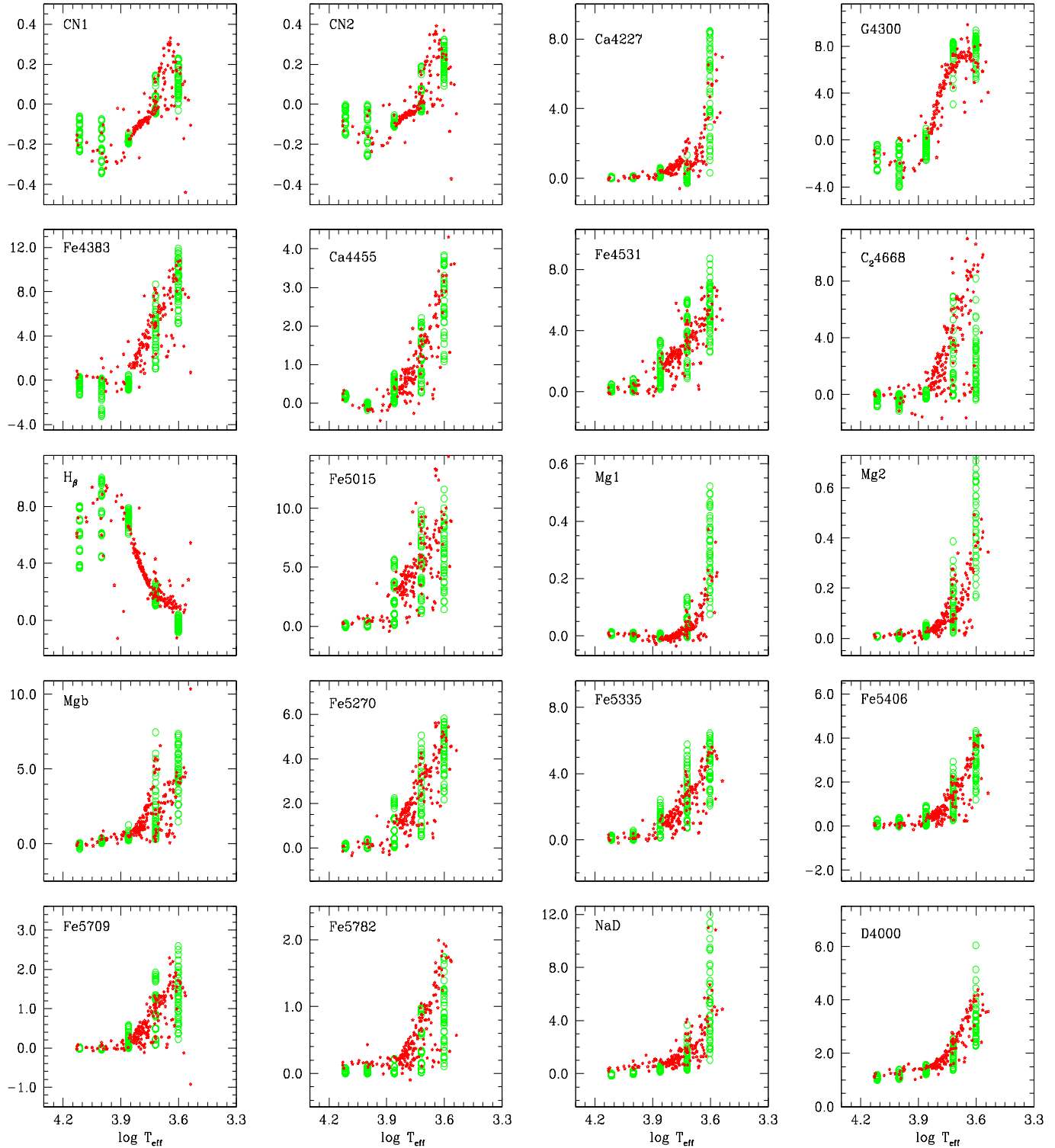


**Figure 11.** Comparison of 19 indices on the Lick system plus D4000 measured on a selected sample of stars of STELIB, for which the atmospheric parameters are known and the spectrum is complete, with the indices derived from theoretical 1 Å resolution spectra of the whole  $T_{\text{eff}}$ ,  $\log g$  and  $[\text{Fe}/\text{H}]$  grid adopted in this work. The small dots are the STELIB objects whereas the open circles are the theoretical spectra. The comparison is made as a function of  $T_{\text{eff}}$ .

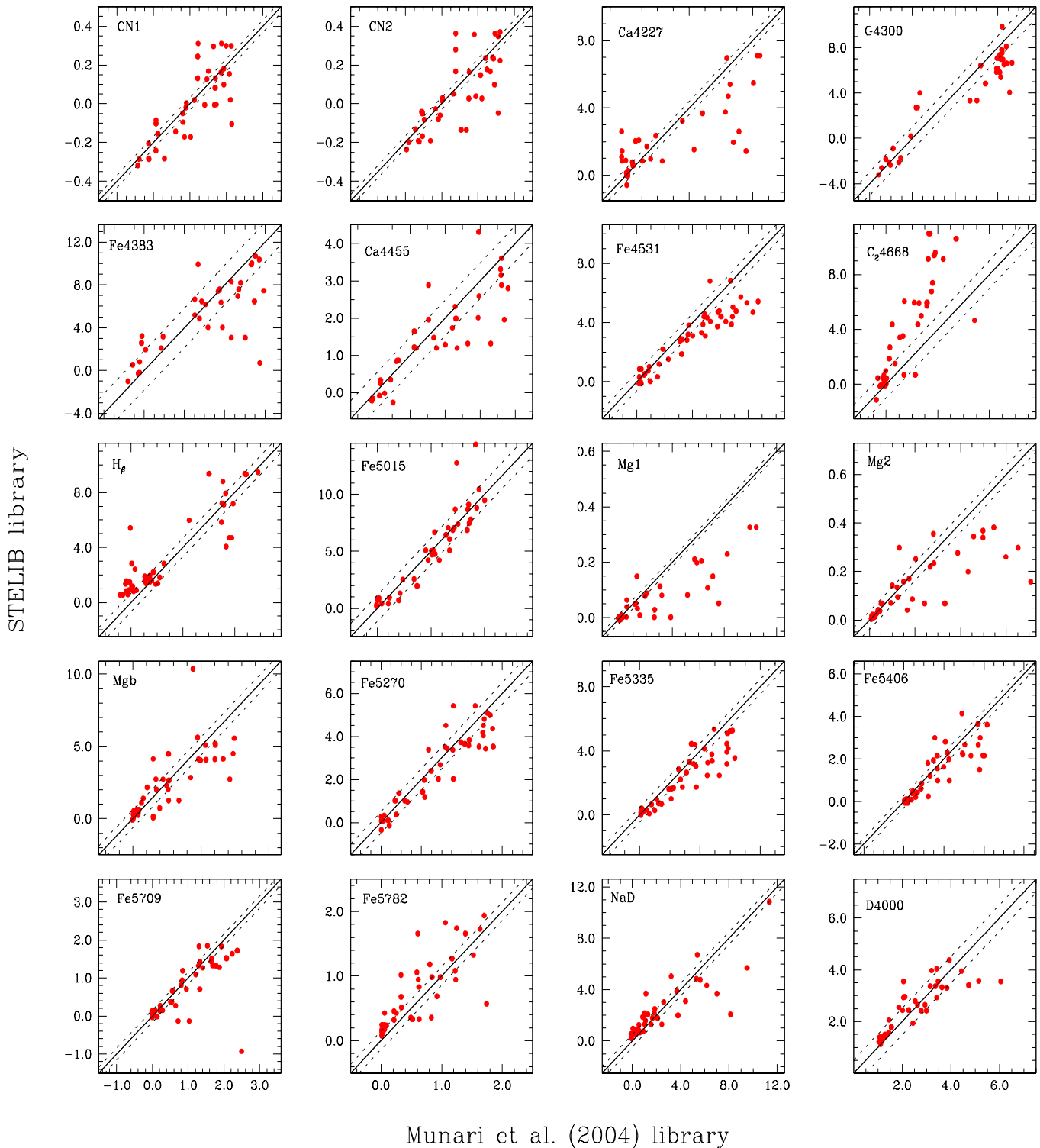


**Figure 12.** Index-index comparison between the value measured from the theoretical spectra of the Munari et al. (2004) library and the one derived from stars of STELIB selected to have the closest matches of the  $T_{\text{eff}}$ ,  $\log g$  and  $[\text{Fe}/\text{H}]$  of our library. The transverse solid and dotted lines show the loci of equality and  $\pm 20\%$  uncertainty.

underlying scatter in  $\log g$  and  $[\text{Fe}/\text{H}]$  and the coarse grid of  $T_{\text{eff}}$ s for the theoretical spectra, the agreement is fairly good.

Fig. 12 compares index-by-index the results obtained from STELIB (y axis) and our library of theoretical spec-

tra (x axis) for the reference stars. In each panel the dotted diagonal lines define the strip of 20 % uncertainty with respect to equality. The scatter can be accounted for by (i) the coarse association of the three parameters ( $\log T_{\text{eff}}$ ,  $\log g$ , and  $[\text{Fe}/\text{H}]$ ), the slightly different resolution of the STELIB

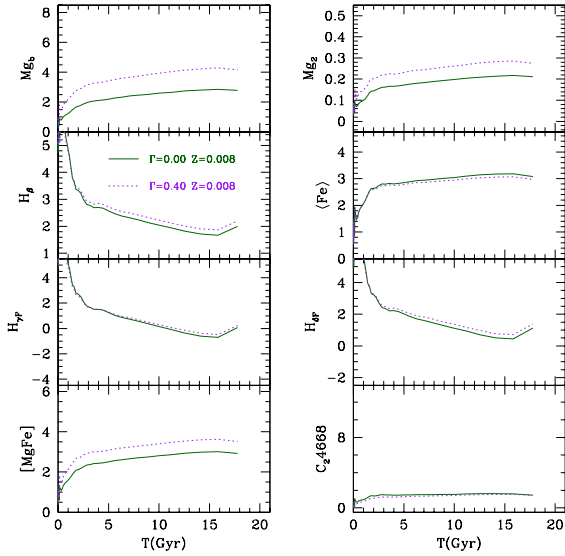


**Figure 13.** Indices straight from 1 Å resolution spectra: the temporal variation of indices. No use of  $\mathcal{FF}$ s and  $\mathcal{RF}$ s is made. The metallicity is  $Z=0.008$ . The thin lines are for  $\Gamma=0$ , whereas the thick lines are for  $\Gamma=0.25$ .

(3 Å) and our spectra (1 Å), and (iii) perhaps real difference in the chemical parameters passing from data to theory.

## 5.2 Indices for SSPs

In this section we derive the Lick indices for SSPs. Since extrapolating spectra out of the parameter range for which they have been calculated may be risky, the analysis is limited to the metallicities in the range  $Z=0.0004$  to  $Z=0.008$ , i.e.  $[Z/Z_\odot]=-2.0$  to  $-0.5$  and  $\Gamma=0$  to  $\Gamma=0.25$ .

To derive the spectral energy distribution of a SSP we apply the standard population synthesis technique (see Bressan et al. 1994, for all details). In brief, along each elemental bin of an isochrone (characterized by  $\log T_{\text{eff}}$ ,  $\log g$ , and the relative number of stars  $dN$ ) we associate the spectrum derived from linearly interpolating the 1 Å resolution spectral grid. Then we sum up all elemental contributions along the isochrone weighed on the relative number of stars and luminosity of the bin. The SSP spectrum is filtered with the pass-bands for each index according to its definition to derive  $F_{l,i}$  and  $F_{c,i}$  for each elemental bin and finally eqn. (15) is applied to get the total index.

The results are shown in Fig. 13, which displays the temporal evolution of the indices  $H_\beta$ ,  $H_\gamma F$ ,  $H_\delta F$ ,  $\langle Fe \rangle$ ,  $Mg_b$ ,  $Mg_2$ ,  $[MgFe]$ , and  $C_{24668}$ , and in Fig. 14, which is the analog of Fig. 8 limited to the sub-solar metallicities ( $Z \leq 0.008$ ). First of all it is evident that the new indices share the same trends of the old ones thus lending internal consistency to the whole problem. Secondly, the effects of enhancement are in agreement with the expectation for the metallicities in use. Thirdly despite the limited and coarse coverage of the spectral library in the temperature-gravity space the results seem to be adequate. However, no comparison with the observational data can be made because they should be obtained with the same resolution as the theoretical indices.

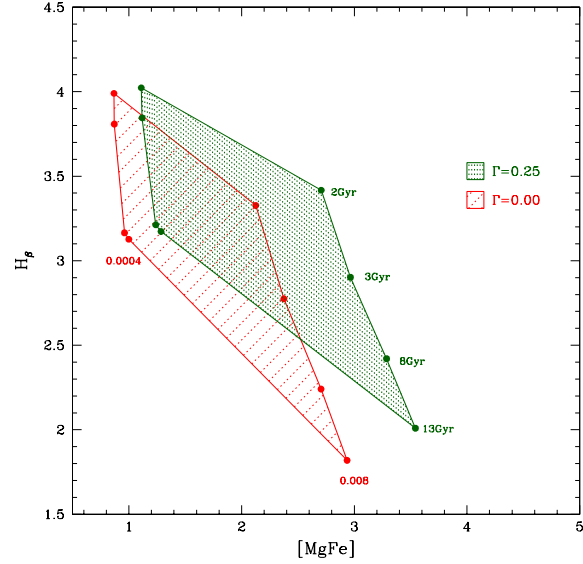


**Figure 14.** Indices straight from 1 Å resolution spectra: the  $H_\beta$  vs.  $[MgFe]$  plane. No use of  $\mathcal{FF}$ s and  $\mathcal{RF}$ s is made. The metallicity goes from  $Z=0.0004$  to  $Z=0.008$  ( $[Z/Z_\odot]=-2.0$  to  $[Z/Z_\odot]=-0.5$ ). This is the analogue of Fig. 8 however limited to sub-solar metallicities. The effect of the  $\alpha$ -enhancement on  $H_\beta$  is once more confirmed and in addition to this the dependence on the metallicity is highlighted. The correction  $\delta H_\beta = H_{\beta \text{enh}} - H_{\beta \text{sol}}$  increases with the metallicity. The various symbols are the same as in Fig. 8. In this case no comparison with observational data can be made because the theoretical indices are from spectra with 1 Å resolution and no data are yet available at the same resolution.

However, there are systematic differences. Looking at metallicity  $Z=0.008$  in common between the SSPs displayed in Fig. 8 and those of Fig. 14 we note:

- (i) for the solar-scaled mixture ( $\Gamma=0$ ) at the age of 2 Gyr  $\Delta H_\beta=0.0$  and  $\Delta [MgFe]=0.45$  passing from the indices with the old  $\mathcal{FF}$ s and the new  $\mathcal{RF}$ s to those straight from the spectra, at the age of 13 Gyr the same differences amount to  $\Delta H_\beta=0.20$  and  $\Delta [MgFe]=0.15$ ;
- (ii) for  $\alpha$ -enhanced mixture ( $\Gamma=0.25$ ) at age of 2 Gyr  $\Delta H_\beta=-0.05$  and  $\Delta [MgFe]=0.45$ , whereas at the age of 13 Gyr the same differences amount to  $\Delta H_\beta=0.10$  and  $\Delta [MgFe]=0.20$ . Whether these differences are real or due to the coarse grids in  $T_{\text{eff}}$  and  $\log g$  cannot be assessed at the present time. Work is in progress to calculate indices with a finer spacing in temperature and gravity and a range of different resolutions.

## 6 DISCUSSION AND CONCLUSIONS

We have generated synthetic absorption line indices on the Lick system based on the recent library of 1 Å resolution spectra calculated by Munari et al. (2004) over a large range of  $\log T_{\text{eff}}$ ,  $\log g$ ,  $[Fe/H]$  and both for solar and  $\alpha$ -enhanced abundance ratios in the chemical composition. The study is made in two steps:

- (i) Firstly we derive a modern version of the so-called  $\mathcal{RF}$ s of TB95. Contrary to the previous situation in which the  $\mathcal{RF}$ s were known only for three stars of given  $T_{\text{eff}}$  and  $\log g$ ,

now the  $\mathcal{RF}$ s are given for large range ranges of  $T_{\text{eff}}$ ,  $\log g$ , and  $[\text{Fe}/\text{H}]$  (or  $[\text{Z}/\text{Z}_\odot]$ ). Not only the  $\mathcal{RF}$ s vary with the type of star but also with the metallicity<sup>6</sup>. The effect of metallicity is important and cannot be neglected.

ii) With the aid of the new  $\mathcal{RF}$ s and the  $\mathcal{FF}$ s of Worthey et al. (1994) indices for SSPs are calculated and compared with the old ones by TC04a. But for the differences caused by the new  $\mathcal{RF}$ s, the agreement is good thus confirming that the method adopted by TC04a to correct for the effect of  $\alpha$ -enhancement albeit hampered by the coarse grid of calibrating stars in TB95 was correct. These results clearly demonstrate that not only all indices depend on the enhancement but also that  $H_\beta$  increases with it as already anticipated by TC04a and contrary to what claimed by Thomas et al. (2003a,b). Furthermore, all this lends strong support to the suggestion made by Tantalo & Chiosi (2004b) that a significant part of the scatter along the  $H_\beta$  axis shown by galaxies in the  $H_\beta$  vs.  $[\text{Mg}/\text{Fe}]$  plane (and similar) could be due to a spread in the mean enhancement factor from galaxy to galaxy and only occasionally to recent episodes of star formation.

iii) Secondly we present preliminary synthetic indices on the Lick system directly measured on theoretical 1 Å resolution spectra. The analysis is considered to be preliminary because much narrower spacing in  $T_{\text{eff}}$  and  $\log g$  than the one for the subset of the Munari et al. (2004) library to our disposal is indeed required. Work is in progress to include the desired spacing in  $T_{\text{eff}}$  and  $\log g$ . Nevertheless the results obtained in so far are satisfactory because the overall dependence on the main parameters of the problem, i.e. chemical composition, degree of enhancement and age are recovered. Finally, we plan to provide in a forthcoming paper (Tantalo & Chiosi 2004c) libraries of theoretical indices based on spectra with same resolution of the observational ones so that comparison with the wealth of data coming from modern spectro-photometric surveys, e.g. SLOAN, is possible.

As a conclusion, given that the absorption line indices proved to be useful tools to infer the age, metallicity and degree of enhancement of composite stellar populations, there is no reason to abandon them. However the present day availability of large libraries of theoretical and empirical spectra at high resolution together with fast numerical techniques make obsolete the use of the  $\mathcal{FF}$ s and  $\mathcal{RF}$ s, which have always been sources of uncertainty. Nevertheless, recalling that all indices of the Lick system stand on the ratio  $F_l/F_c$ , which is equivalent to a narrow band colour, it would be better to define all of them in the classical way, i.e. on a magnitude scale. The present day definition part in pseudo equivalent width and part in magnitude is often cause of misunderstanding.

<sup>6</sup> The new  $\mathcal{RF}$ s are given as large 3D-matrices made available on the web page <http://dipastro.pd.astro.it/galadriel>.

*Qu'à la fin de l'envoi je touche!*

*Cyrano de Bergerac*

*Edmond Rostand (1868 – 1918)*

## ACKNOWLEDGEMENTS

This study has been financed by the Italian Ministry of Education, University, and Research (MIUR), and the University of Padua under the special contract “Formation and evolution of elliptical galaxies: the age problem”.

## REFERENCES

Anders E., Grevesse N., 1989, *Geochim. Cosmochim. Acta*, 53, 197  
 Barbuy B., 1994, *ApJ*, 430, 218  
 Bertelli G., Bressan A., Chiosi C., Fagotto F., Nasi E., 1994, *A&AS*, 106, 275  
 Borges C. A., Idiart T. P., de Freitas-Pacheco J. A., Thevein F., 1995, *AJ*, 110, 2408  
 Bressan A., Chiosi C., Fagotto F., 1994, *ApJS*, 94, 63  
 Bressan A., Chiosi C., Tantalo R., 1996, *A&A*, 311, 425  
 Bruzual G., 1983, *ApJ*, 273, 205  
 Burstein D., Bertola F., Buson L. M., Faber S. M., Lauer T. R., 1988, *ApJ*, 328, 440  
 Burstein D., Faber S. M., Gaskell C. M., Krumm N., 1984, *ApJ*, 287, 586  
 Carney B., 1996, *PASP*, 108, 900  
 Castelli F., Kurucz R. L., 2004, in Piskunov N. E., Weiss W. W., Gray D. F., eds, *Modelling of Stellar Atmospheres* IAU Symposium. p. 189  
 Cenarro A. J., Cardiel N., Gorgas J., Peletier R. F., Vazdekis A., Prada F., 2001, *MNRAS*, 326, 959  
 Cenarro A. J., Gorgas J., Cardiel N., Vazdekis A., Peletier R. F., 2002, *MNRAS*, 329, 863  
 Chiosi C., Carraro G., 2002, *MNRAS*, 335, 335  
 Davies R. L., Kuntschner H., Emsellem E., Bacon R., Bureau M., Carollo C. M., Copin Y., Miller B. W., Monnet G., Peletier R. F., Verolme E. K., de Zeeuw P. T., 2001, *ApJL*, 548, L33  
 Faber S. M., Friel E. D., Burstein D., Gaskell C. M., 1985, *ApJS*, 57, 711  
 Faber S. M., Worthey G., González J. J., 1992, in Barbuy B., Renzini A., eds, *The Stellar Population of Galaxies* IAU Symp. 149. Kluwer Academic Publishers: Dordrecht, p. 255  
 Girardi L., Bertelli G., 1998, *MNRAS*, 300, 533  
 Girardi L., Bertelli G., Bressan A., Chiosi C., Groenewegen M., Marigo P., Salasnich B., Weiss A., 2002, *A&A*, 391, 195  
 Girardi L., Bressan A., Bertelli G., Chiosi C., 2000, *A&AS*, 141, 371  
 González J. J., 1993, PhD thesis, University of California, Santa Cruz  
 Gorgas J., Cardiel N., Pedraz S., González J. J., 1999, *A&AS*, 139, 29  
 Gratton R., Carretta E., Claudi R., Lucatello S., Barbieri M., 2003, *A&A*, 404, 187  
 Grevesse N., Sauval A. J., 1998, *Space Sci. Rev.*, 85, 161

Habgood M.-J., 2001, PhD thesis, Univ. of North Carolina at Chapel Hill

Idiart T. P., de Freitas-Pacheco J. A., 1995, AJ, 109, 2218

Jørgensen I., 1999, MNRAS, 306, 607

Kuntschner H., 1998, PhD thesis, Univ. of Durham

Kuntschner H., 2000, MNRAS, 315, 184

Kuntschner H., Davies R. L., 1998, MNRAS, 295, L29

Kuntschner H., Lucey J. R., Smith R. J., Hudson M. J., Davies R. L., 2001, MNRAS, 323, 615

Kurucz R. L., 1993, in *Diatomeric Molecular Data for Opacity Calculations* CD-ROM No. 15

Larson R. B., 1974, MNRAS, 142, 501

Le Borgne J.-F., Bruzual G., Pelló R., Lançon A., Rocca-Volmerange B., Sanahuja B., Schaerer D., Soubiran C., Vílchez-Gómez R., 2003, 402, 433

Longhetti M., Bressan A., Chiosi C., Rampazzo R., 2000, A&A, 353, 917

Longhetti M., Rampazzo R., Bressan A., Chiosi C., 1998, A&AS, 130, 251

Maraston C., Greggio L., Renzini A., S.Ortolani Saglia R., Puzia T., Kissler-Patig M., 2003, A&A, 400, 823

Matteucci F., 1994, A&A, 154, 279

Matteucci F., 1997, Fundam. Cosmic Phys., 17, 283

Matteucci F., Ponzone R., Gibson B. K., 1998, A&A, 335, 855

Munari U., Sordo R., Castelli F., Zwitter T., 2004, A&A, to be submitted

Poggianti B., Bridges T., Mobasher B., Carter D., Doi M., Iye M., Kashikawa N., Komiyama Y., Okamura S., Sekiguchi M., Shimasaku K., Yagi M., Yasuda N., 2001, ApJ, 562, 689

Puzia T., Saglia R., Kissler-Patig M., Maraston C., Greggio L., Renzini A., Ortolani S., 2002, A&A, 395, 45

Reimers D., 1975, Mem. Soc. R. Sci. Liege, ser. 6, 8, 369

Renzini A., Buzzoni A., 1986, in Chiosi C., Renzini A., eds, *Spectral Evolution of Galaxies* Dordrecht: Reidel, p. 213

Ryan S., Norris J., Bessell M., 1991, AJ, 102, 303

Salasnich B., Girardi L., Weiss A., Chiosi C., 2000, A&A, 361, 1023

Sanchez-Blazquez P., et al. 2004, MNRAS, in preparation

Sánchez-Blázquez P., Peletier R., Vazdekis A., Gorgas J., Cardiel N., Selam S., Falcón J., 2003, in Avila-Reese V., Firmani C., Frenk C., Allen C., eds, *Revista Mexicana de Astronomía y Astrofísica Conference Series* Vol. 17. p. 192

Schwenke D. W., 1998, Faraday Discussion, 109, 321

Tantalo R., 1998, PhD thesis, Univ. of Padova

Tantalo R., Chiosi C., 2004a, MNRAS, submitted

Tantalo R., Chiosi C., 2004b, MNRAS, accepted

Tantalo R., Chiosi C., 2004c, MNRAS, in preparation

Tantalo R., Chiosi C., Bressan A., 1998, A&A, 333, 419

Thomas D., Maraston C., 2003, A&A, 401, 429

Thomas D., Maraston C., Bender R., 2003a, MNRAS, 339, 897

Thomas D., Maraston C., Bender R., 2003b, MNRAS, 343, 279

Trager S., 1997, PhD thesis, Univ. of California, Santa Cruz

Trager S. C., Faber S. M., Worthey G., González J. J., 2000a, AJ, 120, 165

Trager S. C., Faber S. M., Worthey G., González J. J., 2000b, AJ, 119, 1645

Trager S. C., Worthey G., Faber S. M., Burstein D., Gonzalez J. J., 1998, ApJS, 116, 1

Tripicco M. J., Bell R. A., 1995, AJ, 110, 3035

Vassiliadis D. A., Wood P. R., 1993, ApJ, 413, 641

Vazdekis A., Kuntschner H., Davies R. L., Arimoto N., Nakamura O., Peletier R. F., 2001, apj, 551, 127

Weiss A., Peletier R. F., Matteucci F., 1995, A&A, 296, 73

Worthey G., 1992, PhD thesis, Univ. of California

Worthey G., 1994, ApJS, 95, 107

Worthey G., Faber S. M., González J. J., 1992, ApJ, 398, 69

Worthey G., Faber S. M., González J. J., Burstein D., 1994, ApJS, 94, 687

Worthey G., Ottaviani D., 1997, ApJS, 111, 377

Zwitter T., Castelli F., Munari U., 2004, A&A, 417, 1055

## APPENDIX A:

The new  $\mathcal{RF}$ s calculated with the 1 Å resolution spectra from Munari et al. (2004) as function of  $T_{\text{eff}}$  and  $\log g$  and for four different metallicities:  $[\text{Z}/\text{Z}_{\odot}] = -2.0, -1.5, -1.0, -0.5$  are displayed in Tables A1, A2, A3, and A4, respectively. For each index we give the value  $I_{\text{sol}}$  for the solar abundance ratios and the difference  $(\delta I) = I_{\text{enh}} - I_{\text{sol}}$  between the  $\alpha$ -enhanced and the solar case. The corresponding  $\mathcal{RF}$  can immediately be derived from relation (14)

**Table A1.**  $I_{enh} - I_{sol}$  calculated for  $[Z/Z_{\odot}] = -2.0$

$T_{\text{eff}}$	4000								5250							
$\log g$	1.5		2.5		3.5		4.5		1.5		2.5		3.5		4.5	
	$I_{\text{sol}}$	$(\delta I)$														
CN1	0.043	0.024	0.057	0.041	0.050	0.044	0.047	0.043	-0.025	0.002	-0.029	0.003	-0.035	0.005	-0.041	0.009
CN2	0.092	0.039	0.129	0.056	0.126	0.062	0.143	0.055	0.001	0.002	-0.009	0.004	-0.022	0.007	-0.034	0.014
Ca4227	0.328	1.228	1.272	1.460	2.213	1.564	3.872	1.296	0.095	0.081	0.042	0.121	0.033	0.209	0.135	0.358
G4300	8.302	-0.881	8.620	-1.429	7.356	-1.431	6.386	-1.885	3.053	0.216	4.441	0.045	5.746	-0.203	6.863	-0.616
Fe4383	5.127	-1.010	5.742	-1.282	5.221	-1.029	5.448	-1.329	1.079	0.086	1.067	0.020	1.270	-0.100	1.700	-0.253
Ca4455	1.208	0.102	1.253	0.105	1.082	0.122	1.141	0.019	0.341	0.055	0.302	0.062	0.278	0.055	0.276	0.053
Fe4531	3.218	0.044	3.025	0.035	2.611	0.098	2.678	0.018	1.276	0.260	1.131	0.253	1.002	0.224	0.888	0.197
C24668	0.705	0.192	0.335	0.144	-0.029	0.174	-0.359	0.165	-0.096	0.116	-0.072	0.091	-0.039	0.075	-0.006	0.079
$H_{\beta}$	0.129	0.065	-0.085	0.026	-0.212	-0.009	-0.296	-0.077	1.666	0.061	1.389	0.042	1.167	0.033	1.046	0.014
Fe5015	3.714	-0.101	2.826	-0.226	2.068	-0.200	1.432	-0.250	1.435	0.267	1.372	0.249	1.285	0.237	1.136	0.231
Mg1	0.076	0.044	0.162	0.062	0.188	0.082	0.272	0.081	-0.004	0.000	-0.003	0.000	-0.004	0.001	-0.004	0.004
Mg2	0.165	0.068	0.303	0.095	0.353	0.124	0.459	0.099	0.022	0.005	0.026	0.009	0.036	0.017	0.057	0.031
Mg <sub>b</sub>	1.966	0.902	3.586	1.133	4.091	1.336	4.374	0.762	0.372	0.151	0.528	0.285	0.959	0.547	1.723	0.955
Fe5270	2.168	0.103	2.555	0.001	2.516	-0.005	2.695	-0.207	0.526	0.158	0.550	0.149	0.606	0.138	0.704	0.126
Fe5335	2.085	0.053	2.294	-0.038	2.201	-0.078	2.437	-0.338	0.762	0.087	0.741	0.090	0.735	0.085	0.769	0.070
Fe5406	1.215	0.010	1.538	-0.074	1.594	-0.086	1.844	-0.287	0.274	-0.022	0.316	-0.015	0.358	-0.001	0.417	0.006
Fe5709	0.652	0.040	0.559	0.028	0.365	0.018	0.227	-0.012	0.085	0.016	0.091	0.016	0.090	0.017	0.077	0.017
Fe5782	0.254	-0.013	0.240	-0.026	0.153	-0.024	0.107	-0.030	0.020	0.000	0.022	0.000	0.022	0.001	0.019	0.001
NaD	1.030	-0.126	1.860	-0.237	2.550	-0.214	4.313	-0.724	0.286	-0.011	0.307	-0.013	0.394	-0.021	0.606	-0.030
TiO1	0.002	0.003	0.002	0.004	0.000	0.005	-0.001	0.003	0.000	0.000	0.000	0.000	0.000	0.000	-0.001	0.000
TiO2	0.015	0.000	0.014	0.002	0.010	0.005	0.006	0.002	0.001	0.000	0.001	0.000	0.001	0.000	0.000	0.000
$H_{\delta A}$	-3.633	1.244	-3.861	1.420	-3.422	1.295	-3.158	1.614	0.759	0.008	0.349	0.040	-0.278	0.119	-1.028	0.212
$H_{\gamma A}$	-7.774	0.086	-9.516	0.809	-8.939	0.900	-9.083	1.805	-1.041	-0.133	-2.589	0.036	-4.228	0.289	-5.810	0.686
$H_{\delta F}$	-1.682	0.282	-1.887	0.409	-1.685	0.455	-1.473	0.689	1.075	0.049	0.750	0.070	0.344	0.113	-0.046	0.150
$H_{\gamma F}$	-3.023	0.287	-3.953	0.688	-3.831	0.761	-3.823	1.129	0.667	0.038	-0.263	0.118	-1.319	0.263	-2.316	0.487
D4000	2.422	-0.130	2.335	-0.184	2.276	-0.152	2.312	-0.200	1.407	0.032	1.380	0.028	1.397	0.028	1.450	0.030

$T_{\text{eff}}$	7250						10000						13000							
$\log g$	1.5		2.5		3.5		4.5		2.5		3.5		4.5		2.5		3.5		4.5	
	$I_{\text{sol}}$	$(\delta I)$																		
CN1	-0.129	0.000	-0.235	0.000	-0.344	0.000	-0.077	0.000	-0.149	0.000	-0.235	0.000	-0.185	0.003	-0.197	0.002	-0.189	0.001	-0.171	0.000
CN2	-0.042	0.000	-0.137	0.000	-0.258	0.000	-0.016	0.000	-0.069	0.000	-0.152	0.000	-0.093	0.003	-0.113	0.002	-0.112	0.001	-0.100	0.000
Ca4227	0.018	0.000	0.010	0.002	0.003	0.006	0.007	0.000	0.006	0.000	0.002	0.000	0.032	0.027	0.044	0.022	0.052	0.020	0.062	0.021
G4300	-0.851	0.018	-2.462	0.020	-3.990	0.017	-0.416	0.000	-1.309	0.001	-2.598	-0.005	-1.320	0.192	-1.669	0.207	-1.704	0.196	-1.534	0.164
Fe4383	-0.175	0.005	-1.023	0.004	-3.234	0.004	0.075	0.003	-0.300	0.004	-1.318	-0.001	-0.166	0.043	-0.658	0.009	-0.860	-0.015	-0.818	-0.031
Ca4455	0.030	-0.020	0.014	-0.021	-0.002	-0.023	0.257	-0.023	0.236	-0.024	0.210	-0.021	-0.006	-0.007	0.017	-0.012	0.038	-0.006	0.048	0.007
Fe4531	0.056	0.004	0.036	0.003	0.026	0.002	0.024	0.002	0.023	0.001	0.017	0.001	0.371	0.058	0.299	0.040	0.233	0.028	0.176	0.024
C <sub>2</sub> 4668	0.052	0.000	0.047	0.000	-0.024	0.001	0.146	0.001	0.123	-0.001	0.099	-0.002	-0.170	0.031	-0.120	0.025	-0.080	0.020	-0.045	0.018
H <sub>β</sub>	6.063	-0.002	8.825	-0.003	9.741	-0.001	3.894	-0.001	6.203	-0.001	8.037	0.005	7.151	0.021	7.134	0.018	6.678	0.015	6.086	0.014
Fe5015	0.059	-0.044	0.043	-0.028	-0.034	-0.017	0.133	-0.059	0.087	-0.053	0.046	-0.039	0.200	0.022	0.164	0.023	0.129	0.023	0.106	0.023
Mg <sub>1</sub>	0.007	0.000	0.004	0.000	-0.007	0.000	0.008	0.000	0.007	0.000	0.003	0.000	0.001	0.000	-0.003	0.000	-0.005	0.000	-0.006	0.000
Mg <sub>2</sub>	0.009	0.000	0.008	0.001	-0.001	0.001	0.009	0.000	0.009	0.000	0.006	0.000	0.014	0.003	0.011	0.002	0.009	0.002	0.009	0.003
Mg <sub>b</sub>	0.066	0.010	0.070	0.021	0.079	0.037	0.034	-0.002	0.035	0.000	0.028	0.001	0.383	0.111	0.384	0.101	0.379	0.093	0.389	0.106
Fe5270	-0.002	0.001	0.002	0.001	0.003	0.001	0.006	0.001	0.007	0.001	0.007	0.001	0.024	0.033	0.052	0.035	0.078	0.036	0.097	0.036
Fe5335	0.020	0.002	0.014	0.002	0.012	0.002	0.012	0.004	0.010	0.002	0.007	0.001	0.170	0.030	0.164	0.029	0.153	0.028	0.141	0.027
Fe5406	0.003	0.001	0.002	0.001	0.002	0.000	0.003	0.001	0.003	0.001	0.003	0.001	0.021	-0.016	0.036	-0.007	0.046	0.000	0.052	0.003
Fe5709	0.002	0.000	0.002	0.000	0.002	0.000	0.002	0.000	0.002	0.000	0.002	0.000	0.003	0.002	0.004	0.003	0.005	0.003	0.005	0.003
Fe5782	0.001	0.000	0.001	0.001	0.001	0.000	0.001	0.000	0.002	0.000	0.001	0.000	0.002	0.000	0.002	0.000	0.002	0.000	0.002	0.000
NaD	-0.031	0.000	-0.013	0.000	0.000	0.000	-0.136	-0.001	-0.102	-0.001	-0.075	-0.001	0.145	-0.001	0.155	-0.001	0.159	-0.001	0.162	-0.002
TiO <sub>1</sub>	0.003	0.000	0.003	0.000	0.003	0.000	0.003	0.000	0.003	0.000	0.002	0.000	0.001	0.000	0.001	0.000	0.001	0.000	0.001	0.000
TiO <sub>2</sub>	0.003	0.000	0.003	0.000	0.003	0.000	0.004	0.000	0.004	0.000	0.004	0.000	0.003	0.000	0.002	0.000	0.001	0.000	0.001	0.000
H <sub>δ</sub> A	6.543	-0.014	11.170	-0.013	15.360	-0.009	4.197	-0.016	7.510	-0.012	11.130	0.012	8.941	-0.026	9.384	-0.003	8.968	0.007	8.118	0.014
H <sub>γ</sub> A	6.628	-0.018	11.270	-0.019	15.520	-0.015	4.152	-0.003	7.445	-0.003	11.140	0.015	8.708	-0.108	9.262	-0.102	8.958	-0.091	8.143	-0.072
H <sub>δ</sub> F	5.935	-0.014	9.009	-0.010	10.460	-0.005	3.837	-0.016	6.380	-0.012	8.434	0.002	7.587	-0.008	7.484	0.004	6.995	0.010	6.332	0.013
H <sub>γ</sub> F	5.969	-0.005	8.880	-0.006	10.300	-0.004	3.885	-0.001	6.304	-0.001	8.291	0.008	7.366	-0.005	7.354	-0.005	6.920	-0.005	6.286	-0.003
D4000	1.080	0.001	1.199	0.001	1.377	0.001	1.017	0.000	1.084	0.000	1.187	0.001	1.217	0.008	1.276	0.007	1.295	0.007	1.294	0.007

**Table A2.**  $I_{enh} - I_{sol}$  calculated for  $[Z/Z_{\odot}] = -1.5$ 

$T_{\text{eff}}$	4000								5250									
	log $g$		1.5		2.5		3.5		4.5		1.5		2.5		3.5		4.5	
	$I_{sol}$	$(\delta I)$																
CN1	0.082	0.007	0.088	0.022	0.072	0.031	0.051	0.030	-0.032	0.001	-0.039	0.003	-0.043	0.006	-0.046	0.013		
CN2	0.150	0.018	0.178	0.030	0.171	0.043	0.158	0.037	-0.006	0.002	-0.018	0.005	-0.029	0.011	-0.038	0.021		
Ca4227	1.041	1.791	2.400	1.764	3.824	1.872	5.133	1.518	0.160	0.143	0.055	0.218	0.050	0.347	0.250	0.556		
G4300	8.389	-0.879	8.376	-1.330	7.356	-1.067	5.699	-1.084	5.157	0.054	6.424	-0.181	7.216	-0.444	8.064	-0.922		
Fe4383	6.349	-1.099	7.111	-1.565	6.858	-1.241	6.265	-1.374	1.685	0.033	1.888	-0.069	2.329	-0.317	2.985	-0.609		
Ca4455	1.751	0.075	1.843	0.046	1.691	0.151	1.538	0.069	0.580	0.015	0.515	0.031	0.465	0.054	0.459	0.067		
Fe4531	4.012	0.037	3.818	-0.004	3.482	0.149	3.317	0.095	2.032	0.268	1.877	0.279	1.713	0.264	1.584	0.236		
C24668	1.390	0.063	0.795	0.141	0.246	0.379	-0.242	0.422	-0.018	0.156	-0.011	0.126	0.014	0.099	0.041	0.096		
$H_{\beta}$	0.093	0.058	-0.200	0.028	-0.395	0.024	-0.476	-0.022	1.787	0.098	1.464	0.090	1.213	0.071	1.056	0.044		
Fe5015	4.747	-0.274	3.736	-0.264	2.934	-0.057	2.134	-0.042	2.497	0.384	2.376	0.362	2.256	0.331	2.119	0.295		
Mg1	0.131	0.048	0.230	0.052	0.279	0.085	0.331	0.087	0.001	0.000	0.001	0.001	0.002	0.001	0.001	0.007		
Mg2	0.241	0.079	0.397	0.090	0.482	0.147	0.531	0.130	0.030	0.007	0.038	0.013	0.057	0.024	0.093	0.045		
$Mg_b$	2.632	1.099	4.334	1.271	5.007	1.750	4.601	1.267	0.308	0.223	0.626	0.419	1.360	0.755	2.590	1.293		
Fe5270	2.849	0.041	3.231	-0.100	3.331	-0.053	3.278	-0.159	0.872	0.241	0.890	0.238	0.983	0.223	1.180	0.200		
Fe5335	2.840	0.008	3.056	-0.154	3.011	-0.139	2.944	-0.331	1.110	0.129	1.115	0.138	1.150	0.138	1.258	0.124		
Fe5406	1.687	-0.022	2.042	-0.166	2.174	-0.134	2.204	-0.259	0.403	0.023	0.457	0.014	0.541	0.011	0.672	0.008		
Fe5709	0.952	0.074	0.830	0.055	0.613	0.061	0.378	0.015	0.210	0.037	0.220	0.038	0.220	0.037	0.203	0.036		
Fe5782	0.491	-0.033	0.468	-0.066	0.339	-0.066	0.220	-0.072	0.055	0.003	0.061	0.003	0.062	0.003	0.058	0.003		
NaD	1.563	-0.180	2.744	-0.398	3.994	-0.308	5.614	-0.695	0.332	-0.027	0.379	-0.036	0.542	-0.062	0.910	-0.095		
TiO <sub>1</sub>	0.006	0.004	0.005	0.007	0.005	0.015	0.002	0.014	0.000	0.000	0.000	0.000	0.000	0.000	0.000	0.000		
TiO <sub>2</sub>	0.025	0.001	0.024	0.007	0.022	0.021	0.014	0.018	0.004	0.001	0.003	0.003	0.001	0.002	0.001	0.001		
$H_{\delta A}$	-5.011	1.471	-5.262	1.690	-4.782	1.360	-3.510	1.324	0.258	0.065	-0.193	0.158	-0.932	0.312	-1.945	0.496		
$H_{\gamma A}$	-9.139	0.177	-10.690	0.988	-10.540	0.684	-9.443	1.217	-2.950	-0.006	-4.475	0.236	-5.746	0.523	-7.302	1.026		
$H_{\delta F}$	-2.400	0.217	-2.641	0.426	-2.425	0.418	-1.727	0.553	0.774	0.089	0.489	0.136	0.094	0.208	-0.382	0.291		
$H_{\gamma F}$	-3.279	0.293	-4.072	0.648	-4.115	0.552	-3.576	0.699	-0.039	0.117	-1.045	0.272	-1.959	0.446	-2.947	0.726		
D4000	2.633	-0.131	2.571	-0.223	2.548	-0.197	2.448	-0.193	1.487	0.052	1.456	0.040	1.484	0.031	1.565	0.025		

$T_{\text{eff}}$	7250								10000								13000							
	log $g$		1.5		2.5		3.5		4.5		2.5		3.5		4.5		2.5		3.5		4.5			
	$I_{sol}$	$(\delta I)$																						
CN1	-0.181	0.003	-0.195	0.002	-0.188	0.002	-0.171	0.001	-0.127	0.000	-0.343	0.001	-0.075	0.000	-0.146	0.000	-0.233	0.000	-0.067	0.000	-0.150	0.000	-0.067	0.000
CN2	-0.088	0.003	-0.110	0.002	-0.099	0.001	-0.041	0.000	-0.134	0.000	-0.256	0.001	-0.015	0.000	-0.067	0.000	-0.150	0.000	-0.015	0.000	-0.067	0.000	-0.015	0.000
Ca4227	0.061	0.035	0.070	0.030	0.080	0.026	0.094	0.030	0.033	0.001	0.022	0.004	0.016	0.014	0.016	0.001	0.015	0.000	0.008	0.000	0.015	0.000	0.008	0.000
G4300	-1.061	0.215	-1.396	0.233	-1.435	0.245	-1.296	0.240	-0.799	0.042	-2.396	0.047	-3.966	0.045	-0.415	-0.006	-1.284	-0.007	-2.571	-0.004	-0.067	0.000	-2.571	-0.004
Fe4383	0.124	0.090	-0.457	0.041	-0.740	0.008	-0.769	-0.024	-0.139	0.013	-0.970	0.009	-3.164	0.007	0.087	0.011	-0.279	0.009	-1.288	0.004	-0.027	0.000	-1.288	0.004
Ca4455	0.016	0.038	0.031	0.018	0.061	0.000	0.090	-0.003	0.001	-0.010	-0.013	-0.014	-0.030	-0.019	0.022	-0.016	0.027	-0.017	0.0184	-0.021	-0.046	0.004	-0.046	0.003
Fe4531	0.661	0.119	0.558	0.099	0.457	0.074	0.374	0.055	0.113	0.009	0.081	0.008	0.062	0.006	0.046	0.007	0.046	0.004	0.032	0.003	0.032	0.003	0.032	0.003
C24668	-0.277	0.077	-0.210	0.056	-0.144	0.038	-0.080	0.030	-0.007	-0.001	0.011	0.001	-0.043	0.004	0.096	0.003	0.094	-0.001	0.083	-0.001	0.083	-0.001	0.083	-0.001
$H_{\beta}$	7.225	0.044	7.213	0.036	6.761	0.029	6.170	0.026	6.015	0.008	8.781	-0.001	9.752	0.000	10.833	0.023	6.134	0.019	7.986	0.009	0.050	0.000	0.047	0.004
Fe5015	0.402	0.061	0.377	0.062	0.345	0.061	0.319	0.059	0.038	-0.067	0.041	-0.051	-0.022	-0.038	0.091	-0.074	0.049	-0.078	0.019	-0.069	0.007	-0.069	0.007	
Mg1	-0.001	0.000	-0.005	0.000	-0.007	0.000	-0.007	0.000	0.007	0.000	0.004	0.000	-0.007	0.000	0.007	0.000	0.007	0.000	0.000	0.000	0.000	0.000	0.000	0.000
Mg2	0.018	0.003	0.015	0.003	0.013	0.003	0.013	0.004	0.010	0.001	0.008	0.001	0.001	0.002	0.009	0.000	0.009	0.000	0.006	0.000	0.006	0.000	0.006	0.000
$Mg_b$	0.473	0.104	0.460	0.108	0.448	0.116	0.484	0.161	0.081	0.025	0.108	0.046	0.143	0.064	0.043	-0.005	0.050	0.006	0.003	0.007	0.002	0.007	0.002	0.002
Fe5270	0.110	0.085	0.140	0.089	0.168	0.090	0.193	0.089	-0.012	0.004	-0.005	0.004	0.000	0.005	0.006	0.002	0.006	0.003	0.007	0.002	0.006	0.003	0.007	0.002
Fe5335	0.318	0.059	0.325	0.065	0.318	0.067	0.304	0.068	0.042	0.006	0.032	0.006	0.027	0.006	0.025	0.012	0.020	0.006	0.014	0.004	0.006	0.005	0.004	
Fe5406	0.046	-0.027																						

**Table A3.**  $I_{enh} - I_{sol}$  calculated for  $[Z/Z_{\odot}] = -1.0$ 

$T_{\text{eff}}$	4000								5250									
	$\log g$		1.5		2.5		3.5		4.5		1.5		2.5		3.5		4.5	
	$I_{sol}$	$(\delta I)$																
CN1	0.135	-0.028	0.120	-0.007	0.090	0.007	0.045	0.017	-0.042	-0.001	-0.043	-0.001	-0.041	0.001	-0.040	0.005		
CN2	0.222	-0.021	0.226	-0.005	0.212	0.008	0.164	0.017	-0.017	0.003	-0.022	0.004	-0.024	0.008	-0.025	0.016		
Ca4227	2.303	2.289	3.863	1.913	5.836	1.509	6.731	1.204	0.209	0.293	0.037	0.424	0.053	0.588	0.441	0.803		
G4300	8.401	-0.765	8.144	-1.090	7.652	-0.936	5.594	-0.399	7.032	-0.231	7.585	-0.317	7.819	-0.466	8.264	-0.862		
Fe4383	7.784	-1.286	8.451	-1.812	8.915	-1.924	7.486	-1.569	2.710	-0.224	3.193	-0.448	3.800	-0.788	4.728	-1.297		
Ca4455	2.336	0.044	2.440	0.018	2.460	0.081	2.109	0.093	0.849	0.043	0.782	0.047	0.731	0.070	0.747	0.095		
Fe4531	4.905	0.123	4.668	0.047	4.577	0.116	4.168	0.160	3.000	0.126	2.874	0.111	2.712	0.093	2.604	0.047		
C <sub>2</sub> 4668	2.269	-0.120	1.376	0.305	0.722	0.933	0.103	1.189	0.512	0.007	0.478	-0.020	0.436	-0.029	0.377	0.006		
$H_{\beta}$	0.031	0.056	-0.326	0.087	-0.593	0.167	-0.669	0.157	1.870	0.188	1.539	0.184	1.247	0.177	1.027	0.147		
Fe5015	5.780	-0.174	4.799	-0.036	4.258	0.297	3.256	0.380	4.109	0.297	3.888	0.266	3.713	0.191	3.618	0.047		
Mg1	0.195	0.042	0.286	0.039	0.370	0.053	0.399	0.078	0.010	0.000	0.009	0.001	0.008	0.003	0.009	0.013		
Mg2	0.331	0.085	0.482	0.091	0.624	0.123	0.630	0.149	0.045	0.009	0.056	0.017	0.085	0.031	0.142	0.060		
Mg <sub>b</sub>	3.380	1.399	4.998	1.537	6.022	1.785	5.153	1.706	0.306	0.337	0.795	0.593	1.852	1.010	3.595	1.640		
Fe5270	3.586	-0.068	3.870	-0.218	4.204	-0.254	4.004	-0.186	1.485	0.211	1.521	0.181	1.690	0.121	2.041	0.039		
Fe5335	3.744	-0.094	3.899	-0.308	4.054	-0.433	3.670	-0.451	1.650	0.090	1.738	0.076	1.873	0.030	2.138	-0.045		
Fe5406	2.272	-0.113	2.584	-0.267	2.894	-0.320	2.728	-0.293	0.706	-0.011	0.772	-0.025	0.918	-0.073	1.188	-0.145		
Fe5709	1.324	0.100	1.161	0.077	0.950	0.074	0.607	0.061	0.488	0.017	0.499	0.012	0.500	0.004	0.479	-0.005		
Fe5782	0.833	-0.065	0.775	-0.123	0.626	-0.170	0.401	-0.167	0.136	0.014	0.150	0.013	0.155	0.010	0.153	0.008		
NaD	2.448	-0.294	3.908	-0.596	6.147	-0.879	7.656	-0.994	0.423	-0.051	0.513	-0.076	0.765	-0.119	1.309	-0.172		
TiO <sub>1</sub>	0.011	0.007	0.011	0.017	0.016	0.034	0.012	0.040	0.002	0.001	0.002	0.001	0.002	0.001	0.001	0.001		
TiO <sub>2</sub>	0.039	0.006	0.038	0.022	0.045	0.049	0.035	0.060	0.009	0.000	0.008	0.000	0.007	0.000	0.006	0.000		
$H_{\delta A}$	-7.093	2.026	-6.977	2.119	-6.823	1.896	-4.447	1.107	-0.614	0.281	-1.117	0.517	-1.995	0.849	-3.473	1.364		
$H_{\gamma A}$	-10.740	0.212	-11.950	1.021	-12.810	1.101	-10.640	0.785	-4.985	0.303	-5.887	0.434	-6.744	0.681	-8.246	1.295		
$H_{\delta F}$	-3.441	0.244	-3.515	0.465	-3.443	0.555	-2.226	0.431	0.342	0.170	0.139	0.249	-0.224	0.374	-0.844	0.585		
$H_{\gamma F}$	-3.662	0.297	-4.236	0.569	-4.582	0.554	-3.715	0.360	-0.751	0.283	-1.488	0.387	-2.161	0.524	-3.076	0.824		
D4000	2.938	-0.121	2.847	-0.243	2.905	-0.284	2.655	-0.201	1.649	0.056	1.617	0.022	1.662	-0.008	1.790	-0.047		

$T_{\text{eff}}$	7250								10000								13000							
	$\log g$		1.5		2.5		3.5		4.5		2.5		3.5		4.5		2.5		3.5		4.5			
	$I_{sol}$	$(\delta I)$																						
CN1	-0.173	0.002	-0.191	0.002	-0.184	0.002	-0.169	0.001	-0.125	0.002	-0.229	0.001	-0.342	0.003	-0.073	0.002	-0.144	0.002	-0.231	0.002				
CN2	-0.080	0.003	-0.106	0.002	-0.106	0.002	-0.097	0.001	-0.039	0.002	-0.131	0.002	-0.255	0.003	-0.013	0.001	-0.065	0.002	-0.148	0.002				
Ca4227	0.122	0.022	0.121	0.026	0.123	0.028	0.141	0.038	0.049	-0.007	0.044	-0.002	0.051	0.008	0.041	-0.007	0.040	-0.008	0.029	-0.007				
G4300	-0.758	0.296	-1.086	0.295	-1.093	0.278	-0.933	0.261	-0.729	0.115	-2.310	0.125	-3.928	0.123	-0.431	0.006	-1.281	0.025	-2.554	0.035				
Fe4383	0.328	0.207	-0.313	0.150	-0.620	0.082	-0.694	0.006	-0.057	0.020	-0.861	0.017	-3.055	0.039	0.137	0.000	-0.228	0.012	-1.241	0.030				
Ca4455	0.155	0.054	0.133	0.047	0.125	0.031	0.140	0.010	-0.025	-0.002	-0.037	-0.008	-0.055	-0.017	0.221	-0.026	0.204	-0.030	0.178	-0.036				
Fe4531	1.166	0.103	1.040	0.110	0.896	0.093	0.772	0.065	0.229	-0.004	0.183	-0.006	0.155	-0.011	0.104	0.003	0.105	-0.004	0.081	-0.006				
C <sub>2</sub> 4668	-0.301	0.114	-0.262	0.089	-0.208	0.064	-0.127	0.045	-0.155	0.025	-0.096	0.028	-0.118	0.035	-0.019	0.024	0.007	0.011	0.031	0.006				
$H_{\beta}$	7.340	0.093	7.346	0.069	6.903	0.050	6.320	0.036	5.968	0.018	8.721	0.041	9.760	0.012	3.830	-0.057	6.103	-0.046	7.948	-0.037				
Fe5015	1.061	-0.005	1.057	-0.002	1.006	-0.005	0.952	-0.008	0.026	-0.018	0.036	-0.001	-0.015	-0.080	0.069	-0.103	0.019	-0.122	-0.009	-0.123				
Mg1	-0.002	0.000	-0.005	0.000	-0.007	0.001	-0.008	-0.001	0.006	0.000	0.003	0.000	-0.008	0.001	0.007	0.000	0.007	0.000	0.003	0.000				
Mg2	0.024	0.001	0.021	0.002	0.018	0.002	0.020	0.005	0.010	0.001	0.010	0.002	0.003	0.002	0.009	0.000	0.009	0.000	0.007	0.000				
Mg <sub>b</sub>	0.463	0.122	0.443	0.141	0.446	0.178	0.548	0.287	0.085	0.066	0.149	0.085	0.221	0.083	0.026	-0.005	0.043	0.005	0.057	0.011				
Fe5270	0.387	0.101	0.405	0.123	0.410	0.135	0.419	0.144	-0.010	0.005	-0.011	0.011	-0.003	0.014	0.008	0.004	0.009	0.006	0.009	0.007				
Fe5335	0.593	0.029	0.628	0.048	0.635	0.065	0.630	0.081	0.088	0.007	0.078	0.004	0.078	0.003	0.061	0.020	0.051	0.009	0.037	0.004				
Fe5406	0.129	-0.046	0.181	-0.043	0.223	-0.032	0.251	-0.016	0.023	0.001	0.015	0.002	0.012	0.003	0.019	0.002	0.020	0.003	0.016	0.004				
Fe5709	0.023	0.014	0.040	0.																				

**Table A4.**  $I_{enh} - I_{sol}$  calculated for  $[Z/Z_{\odot}] = -0.5$ 

$T_{\text{eff}}$	4000								5250									
	log $g$		1.5		2.5		3.5		4.5		1.5		2.5		3.5		4.5	
	$I_{sol}$	( $\delta I$ )																
CN1	0.185	-0.062	0.151	-0.040	0.099	-0.020	0.030	0.002	-0.027	-0.016	-0.021	-0.018	-0.019	-0.016	-0.022	-0.009		
CN2	0.284	-0.060	0.267	-0.044	0.235	-0.030	0.164	-0.003	0.000	-0.011	0.004	-0.013	0.005	-0.009	0.003	0.001		
Ca4227	4.300	2.245	5.563	1.656	7.370	0.864	8.053	0.623	0.104	0.641	-0.081	0.814	-0.010	0.979	0.605	1.178		
G4300	8.423	-0.536	8.049	-0.799	7.884	-0.819	6.068	0.276	7.898	-0.220	8.050	-0.286	8.039	-0.439	8.219	-0.822		
Fe4383	9.299	-1.504	9.703	-2.117	10.640	-2.708	9.187	-1.864	3.774	-0.423	4.371	-0.668	5.023	-0.998	6.104	-1.582		
Ca4455	2.945	0.047	3.024	0.022	3.204	-0.004	2.847	0.119	1.178	0.100	1.133	0.085	1.118	0.081	1.176	0.094		
Fe4531	6.042	0.243	5.709	0.060	5.819	-0.113	5.348	0.158	3.951	0.018	3.826	-0.016	3.683	-0.055	3.597	-0.102		
C <sub>2</sub> 4668	3.171	-0.148	2.070	0.981	1.529	2.371	0.943	3.152	1.527	-0.153	1.490	-0.230	1.304	-0.214	1.047	-0.102		
H <sub>β</sub>	-0.097	0.136	-0.429	0.322	-0.680	0.635	-0.797	0.724	2.064	0.222	1.755	0.207	1.436	0.202	1.149	0.182		
Fe5015	7.168	0.229	6.287	0.431	6.154	0.771	5.004	1.307	5.867	0.286	5.495	0.248	5.216	0.139	5.107	-0.089		
Mg <sub>1</sub>	0.258	0.024	0.330	0.014	0.419	0.001	0.465	0.050	0.027	-0.002	0.027	-0.003	0.024	0.002	0.026	0.018		
Mg <sub>2</sub>	0.432	0.088	0.568	0.082	0.728	0.067	0.751	0.135	0.070	0.010	0.085	0.019	0.124	0.039	0.203	0.075		
Mg <sub>b</sub>	4.242	1.854	5.729	1.794	6.816	1.582	5.959	1.768	0.489	0.436	1.105	0.748	2.487	1.248	4.763	1.902		
Fe5270	4.333	-0.207	4.473	-0.376	4.927	-0.545	4.839	-0.270	2.241	0.215	2.280	0.153	2.482	0.078	2.927	-0.015		
Fe5335	4.798	-0.261	4.829	-0.563	5.076	-0.921	4.618	-0.749	2.292	0.110	2.472	0.069	2.701	-0.007	3.097	-0.121		
Fe5406	2.952	-0.220	3.187	-0.371	3.595	-0.536	3.421	-0.340	1.024	-0.030	1.121	-0.042	1.304	-0.097	1.673	-0.196		
Fe5709	1.768	0.096	1.545	0.059	1.320	0.037	0.925	0.104	0.854	0.046	0.847	0.030	0.834	0.014	0.801	-0.002		
Fe5782	1.224	-0.112	1.103	-0.225	0.912	-0.363	0.627	-0.378	0.300	0.035	0.326	0.029	0.335	0.021	0.337	0.012		
NaD	3.782	-0.483	5.376	-0.959	8.272	-1.803	10.170	-1.708	0.604	-0.072	0.738	-0.115	1.093	-0.174	1.855	-0.252		
TiO <sub>1</sub>	0.019	0.021	0.025	0.044	0.043	0.077	0.042	0.100	0.002	0.001	0.002	0.001	0.002	0.001	0.002	0.001		
TiO <sub>2</sub>	0.059	0.026	0.066	0.062	0.091	0.107	0.086	0.143	0.015	0.000	0.013	0.000	0.012	0.000	0.011	-0.001		
H <sub>δ</sub> A	-9.627	2.690	-8.909	2.708	-8.914	2.685	-6.115	1.030	-1.726	0.568	-2.217	0.897	-3.101	1.323	-4.768	1.974		
H <sub>γ</sub> A	-12.710	0.151	-13.440	1.035	-14.850	1.661	-12.740	0.235	-6.216	0.275	-6.763	0.399	-7.451	0.696	-8.910	1.427		
H <sub>δ</sub> F	-4.793	0.438	-4.506	0.653	-4.404	0.845	-3.000	0.400	-0.016	0.165	-0.109	0.254	-0.402	0.408	-1.066	0.681		
H <sub>γ</sub> F	-4.253	0.269	-4.545	0.467	-4.960	0.525	-4.198	-0.050	-1.043	0.347	-1.582	0.399	-2.147	0.536	-2.979	0.850		
D4000	3.370	-0.128	3.158	-0.263	3.235	-0.375	2.936	-0.218	1.894	0.070	1.821	0.030	1.857	-0.013	2.017	-0.077		

$T_{\text{eff}}$	7250								10000								13000					
	log $g$		1.5		2.5		3.5		4.5		2.5		3.5		4.5		2.5		3.5		4.5	
	$I_{sol}$	( $\delta I$ )																				
CN1	-0.164	0.001	-0.188	0.001	-0.183	0.001	-0.171	0.001	-0.123	0.004	-0.228	0.004	-0.341	0.006	-0.070	0.003	-0.141	0.003	-0.227	0.003	-0.144	0.003
CN2	-0.071	0.002	-0.102	0.001	-0.103	0.002	-0.098	0.001	-0.037	0.003	-0.129	0.005	-0.253	0.006	-0.011	0.002	-0.062	0.003	-0.144	0.003	-0.008	0.008
Ca4227	0.179	0.017	0.165	0.033	0.159	0.049	0.185	0.077	0.043	-0.004	0.046	0.006	0.070	0.006	0.057	-0.006	0.056	-0.006	0.047	-0.008	0.007	-0.008
G4300	-0.385	0.353	-0.707	0.337	-0.679	0.311	-0.466	0.274	-0.622	0.173	-2.186	0.206	-3.831	0.213	-0.442	-0.007	-1.256	0.028	-2.502	0.050	-0.008	0.008
Fe4383	0.474	0.223	-0.194	0.189	-0.488	0.126	-0.549	0.010	0.027	0.057	-0.723	0.054	-2.892	0.099	0.200	0.010	-0.154	0.028	-1.142	0.048	-0.007	0.007
Ca4455	0.345	0.062	0.305	0.044	0.260	0.034	0.229	0.026	-0.048	-0.008	-0.062	-0.018	-0.081	-0.033	0.199	-0.012	0.187	-0.018	0.160	-0.031	-0.008	0.008
Fe4531	1.769	0.113	1.655	0.149	1.476	0.164	1.302	0.152	0.373	0.009	0.320	0.000	0.286	0.015	0.179	0.015	0.183	0.007	0.149	0.001	-0.007	0.007
C <sub>2</sub> 4668	-0.189	0.112	-0.174	0.084	-0.173	0.063	-0.131	0.050	-0.363	0.027	-0.252	0.038	-0.225	0.058	-0.195	0.039	-0.147	0.014	-0.080	0.007	-0.007	0.007
H <sub>β</sub>	7.475	0.137	7.506	0.118	7.085	0.099	6.512	0.083	6.012	-0.004	8.802	-0.022	9.835	-0.041	3.760	-0.066	6.024	-0.058	7.885	-0.059	-0.008	0.008
Fe5015	2.144	0.010	2.125	0.029	2.005	0.031	1.876	0.027	0.028	-0.124	0.031	-0.116	-0.010	-0.117	0.059	-0.101	-0.019	-0.135	-0.068	-0.159	-0.008	0.008
Mg <sub>1</sub>	0.001	-0.001	-0.003	-0.001	-0.006	-0.002	-0.007	-0.002	0.007	-0.001	0.003	0.000	-0.009	0.001	0.008	-0.001	0.007	-0.001	0.003	0.000	-0.001	0.001
Mg <sub>2</sub>	0.030	0.000	0.026	0.001	0.025	0.003	0.029	0.008	0.012	0.002	0.012	0.002	0.005	0.002	0.009	-0.001	0.009	0.000	0.007	0.001	0.000	0.001
Mg <sub>b</sub>	0.361	0.145	0.340	0.174	0.403	0.242	0.666	0.434	0.113	0.106	0.214	0.108	0.297	0.093	-0.031	0.000	0.005	0.017	0.045	0.033	0.008	0.008
Fe5406	0.269	-0.023	0.326	-0.029	0.378	-0.032	0.426	-0.015	0.064	-0.003	0.043	0.003	0.034	0.008	0.049	0.003	0.054	0.006	0.043	0.010	-0.009	0.009
Fe5709	0.063	0.033	0.106	0.033	0.131	0.029	0.142	0.021	-0.004	0.004	-0.001	0.003	0.002	0.004	-0.002	0.005	-0.001	0.005	0.000	0.003	0.000	0.003
Fe5782	0.038	0.003	0.038	0.006	0.037	0.008	0.037	0.009	0.022	-0.010	0.013	-0.005	0.008	-0.002	0.017	-0.014	0.018	-0.013	0.013	-0.009	0.009	0.009
NaD	0.284	-0.003	0.278	-0.011	0.276	-0.017	0.303	-0.023	0.016	-0.010	0.055	-0.006	0.100	-0.008	-0.126	-0.012	-0.097	-0.011	-0.071	-0.007	-0.008	0.008
TiO <sub>1</sub>	0.003	0.000	0.00																			